ABSTRACT

GAUGER, KELLY ANN. Synthesis of Novel Chlorins and Carotenoid-Porphyrin Dyads. (Under the Direction of Dr. Jonathan S. Lindsey.)

The first part of this thesis discusses the synthesis of chlorins bearing electron donating groups in the 3-position. A 3-dimethylaminochlorin **ZnC-(NMe$_2$)^{3}M^{10}** was synthesized in 49% yield, a 3-methoxychlorin **ZnC-OMe^{3}M^{10}** was synthesized in 19% yield, and a 3-methylthiochlorin was synthesized in 95% yield from the corresponding 3-bromochlorin. For **ZnC-(NMe$_2$)^{3}M^{10}** and **ZnC-SMe^{3}M^{10}**, the B band and the Q_y band were bathochromically shifted relative to the benchmark chlorin **ZnC-M^{10}**, and the intensity of the Q_y band increased relative to the B band. However, for **ZnC-OMe^{3}M^{10}**, the B band and the Q_y band were hypsochromically shifted relative to the benchmark chlorin **ZnC-M^{10}**, and the intensity of the Q_y band decreased relative to the B band. Therefore, the effects of electron donating groups on the chlorin macrocycle are not as clear as for electron withdrawing groups, which produce a bathochromic shift of the B and Q_y bands and an increase in the intensity of the Q_y band relative to the B band.

The second part of this thesis discusses the synthesis of carotenoid-porphyrin dyads in a facile manner by performing an aldol condensation using microwave irradiation. These carotenoid-porphyrin dyads can be synthesized using the commercially available *trans*-β-apo-8′-carotenal in yields of 47-48%. In each case, the ^{1}H NMR spectrum indicates that the newly formed double bond is of the (*E*) configuration. The absorption spectrum for each carotenoid-porphyrin dyad shows characteristic features of the benchmark carotenoid and the corresponding benchmark porphyrin. Additionally, a decrease in fluorescence emission

intensity of each carotenoid-porphyrin dyad versus that of the corresponding benchmark porphyrin was observed.

Synthesis of Novel Chlorins and Carotenoid-Porphyrin Dyads

by
Kelly Ann Gauger

A thesis submitted to the Graduate Faculty of
North Carolina State University
in partial fulfillment of the
requirements for the Degree of
Master of Science

Chemistry

Raleigh, North Carolina

2009

APPROVED BY:

Alexander Deiters	Christian Melander
Jonathan S. Lindsey Chair of the Advisory Committee	David A. Shultz

DEDICATION

This work is dedicated to my husband, Kevin Gauger, and my parents, Lance and Candy Gidcumb.

BIOGRAPHY

The author, Kelly Ann Gauger, was born in Anchorage, Alaska. She is the eldest child of Lance and Candice Gidcumb. After graduating from Bartlett High School in Anchorage, she attended Wake Forest University in Winston-Salem, North Carolina, where she obtained a B.S. in biology and a B.A. in chemistry. Following graduation from Wake Forest University, Kelly worked for three years as an analytical chemist at Cardinal Health (formerly Magellan Laboratories).

In the fall of 2003, Kelly began her legal studies at Wake Forest University School of Law in Winston-Salem, North Carolina. While in law school, Kelly served as Articles Editor for the *Wake Forest University Intellectual Property Law Journal* and was active in the Intellectual Property Law Association, holding the position of Vice President. She also worked as a summer associate at Red Hat, Inc., and MacCord Mason, PLLC. Kelly passed the North Carolina Bar Exam in July 2006 and is currently a patent attorney. She married her husband, Kevin Gauger, in August 2006.

Kelly joined the North Carolina State University Department of Chemistry in the fall of 2006. She began her research under the supervision of Dr. Jonathan S. Lindsey in January 2007.

ACKNOWLEDGEMENTS

I thank Dr. Jonathan Lindsey for allowing me to conduct research in his laboratory. I have learned a significant amount from my time in the laboratory. I would also like to thank my committee members: Alexander Deiters, Christian Melander, and David Shultz for their support of my research education.

I thank the past and present members of the Lindsey group. I would especially like to thank Dr. Marcin Ptaszek and Dr. Thiagarajan Balasubramanian for their help and counsel. I am also grateful to Ann Norcross for her assistance. I would also like to thank the staff of the chemistry department, especially Dr. Sabapathy Sankar and Matthew Lyndon.

I also thank my parents for inspiring my love of learning, and for their constant support and encouragement. I would like to thank my brother, Shaun, for always making me laugh. I am also grateful to my husband's family for their support. Finally, I thank my husband, Kevin. I cannot begin to tell you how much your love, understanding, and support has meant to me. I could never have done this without you.

TABLE OF CONTENTS

LIST OF CHARTS

LIST OF FIGURES

LIST OF SCHEMES

LIST OF TABLES

I. Introduction

I.A. Background

1. Structure. Porphyrins, chlorins, and bacteriochlorins are a group of strongly absorbing pigments consisting of a tetrapyrrolic macrocycle that participate in a number of critical processes in nature.[1] Porphyrins are comprised of four pyrrole units joined by methine bridges. Porphyrins are fully conjugated, aromatic, and planar. The macrocycle contains eight α-positions (1, 4, 6, 9, 11, 14, 16, and 19), as well as eight ß-positions (2, 3, 7, 8, 12, 13, 17, and 18) and four *meso* positions (5, 10, 15, and 20).

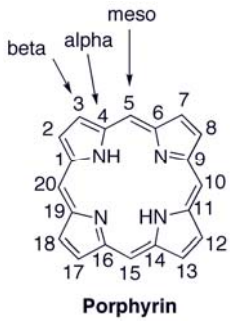

Chart I.1. Structure of porphyrins.

Like porphyrins, chlorins are also aromatic, but possess a reduced pyrrole ring at one of the ß-positions (Chart I.2). Bacteriochlorins are aromatic, and contain two reduced pyrrole rings at the ß-positions on opposite sides of the macrocycle. Isobacteriochlorins are isomers of bacteriochlorins where the two reduced pyrrole rings are on the same side of the macrocycle. Corrins are an example of a non-aromatic, ring-contracted macrocycle.

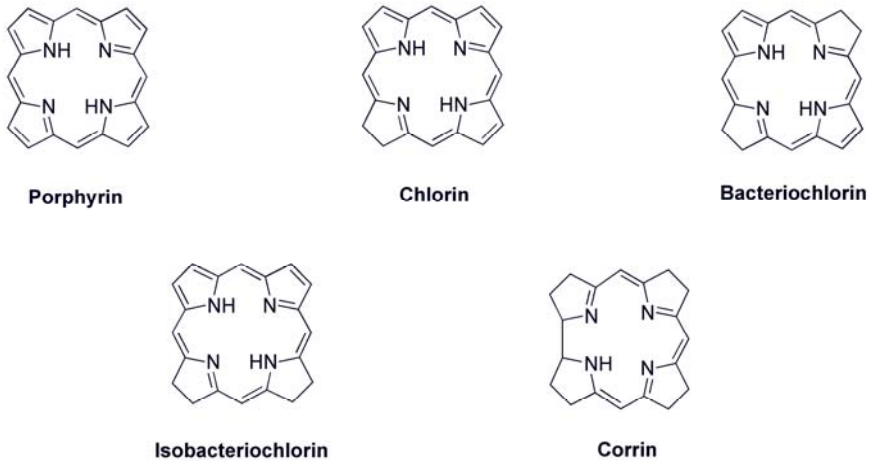

Chart I.2. Structures of a porphyrin, chlorin, bacteriochlorin, isobacteriochlorin, and corrin.

2. Natural Systems. As stated above, porphyrinic molecules participate in a number of critical processes in nature (Chart I.3).[1] For example, hemoproteins contain metalloporphyrin cofactors, which are involved in cellular respiration (cytochromes) as well as the storage and transportation of oxygen (hemoglobin and myoglobin).[2] Additionally, hydroporphyrins (chlorins and bacteriochlorins) form the basis of chlorophylls and bacteriochlorophylls, which play a significant role in photosynthesis.[3] Siroheme, an isobacteriochlorin, plays an important role in the metabolism of sulfur and nitrogen in various organisms.[4] It is a cofactor for sulfite and nitrite reductase, enzymes that reduce sulfite to sulfide and nitrite to ammonia, respectively, in organisms such as *E. coli*.[4] Vitamin B_{12} consists of a corrin macrocycle and is involved in the metabolism of amino acids.[4]

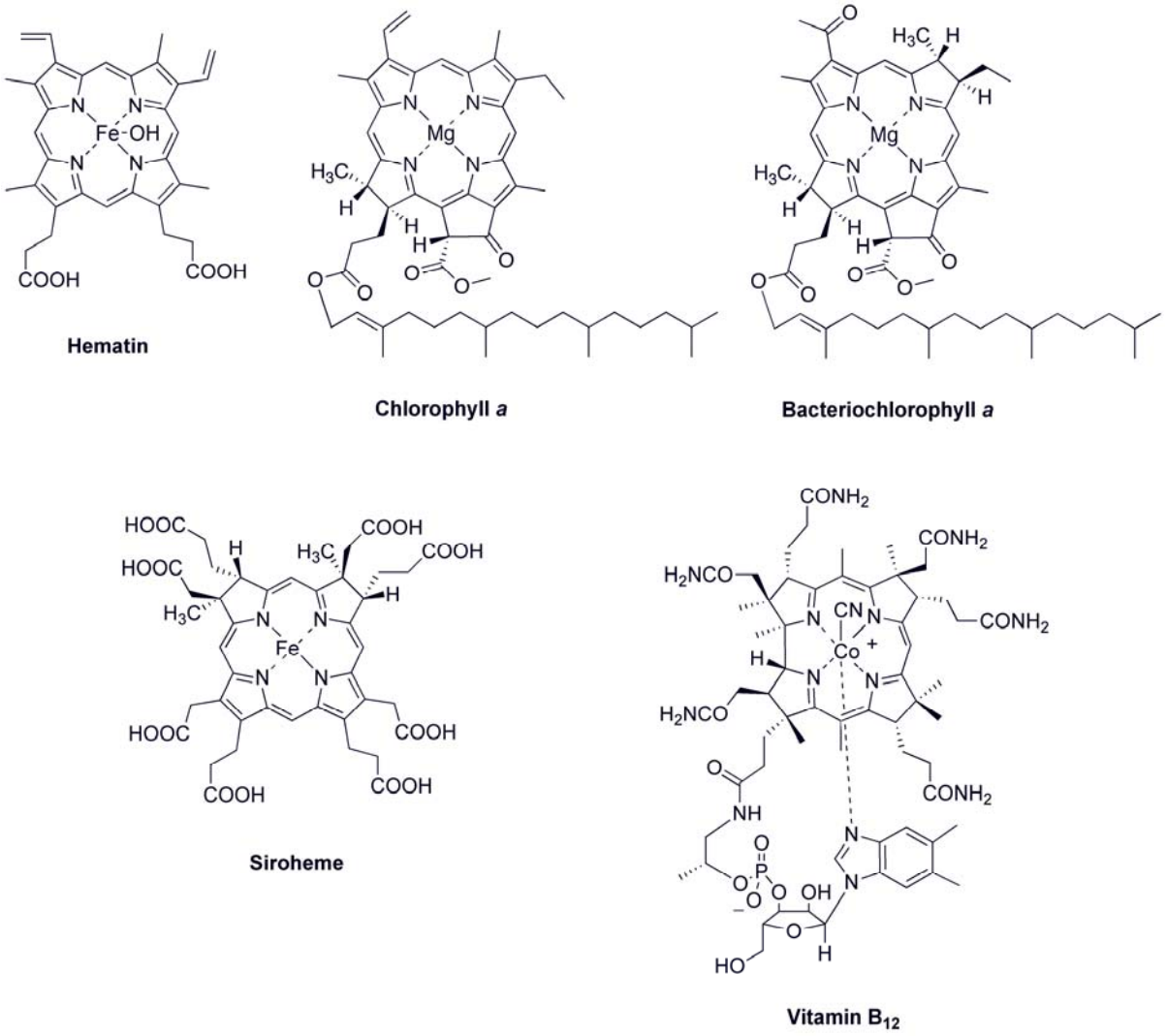

Chart I.3. Structures of naturally occurring porphyrinic molecules.

3. Absorption Spectrocopy. Changes in symmetry and conjugation lead to significant differences in the absorption spectra of porphyrins, chlorins, and bacteriochlorins (Figure I.1). Porphyrins absorb strongly in the near-UV region, with a sharp Soret band (400-450 nm) and weaker Q bands in the visible region (500-650 nm). Chlorins have a B band between 400-450 nm and a Q_y band between 600-650 nm. Bacteriochlorins have the B_x

and B_y bands between 340-370 nm, a Q_x band at approximately 500 nm, and a Q_y band between 700-750 nm. Although chlorins and bacteriochlorins have a slightly weaker absorption in the near-UV region than porphyrins, they possess a greatly enhanced absorption of the Q_y band in the red and near-IR regions, respectively.

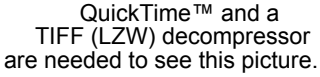

Figure I.1. Absorption spectra of hematin (porphyrin), chlorophyll *a* (chlorin), and bacteriochlorophyll *a* (baceteriochlorin).

4. Synthesis. Due to their presence throughout natural systems and utility in various applications, different synthetic approaches have been developed to prepare porphyrins, chlorins, and bacteriochlorins. Porphyrinic molecules may be prepared by the derivatization

of naturally occurring porphyrins, chlorins, or bacteriochlorins.[5-6] Additionally, hydroporphyrins may be prepared by oxidation or reduction of existing porphyrinic compounds.[7-8] Finally, porphyrinic molecules may be synthesized via a *de novo* route by building the macrocycle from a smaller molecule (such as pyrrole).[9-11]

Chart I.4 shows the syntheses of a porphyrin, chlorin, and bacteriochlorin developed by the Lindsey group. The rational synthesis of ABCD-porphyrins entails acid-catalyzed condensation of a dipyrromethane-1,9-dicarbinol and a dipyrromethane.[9] Chlorins are synthesized by the condensation of a tetrahydrodipyrrin (western half) and bromodipyrromethane-9-carbinol (eastern half) in the presence of acid followed by metal-mediated oxidative cyclization.[10] The synthesis of bacteriochlorins occurs by the Lewis acid catalyzed self-condensation of a dihydrodipyrrin-acetal.[11] Chlorins and bacteriochlorins synthesized via these routes possess geminal dimethyl groups in the reduced rings, preventing adventitious dehydrogenation and thereby imparting additional stability to the compound.

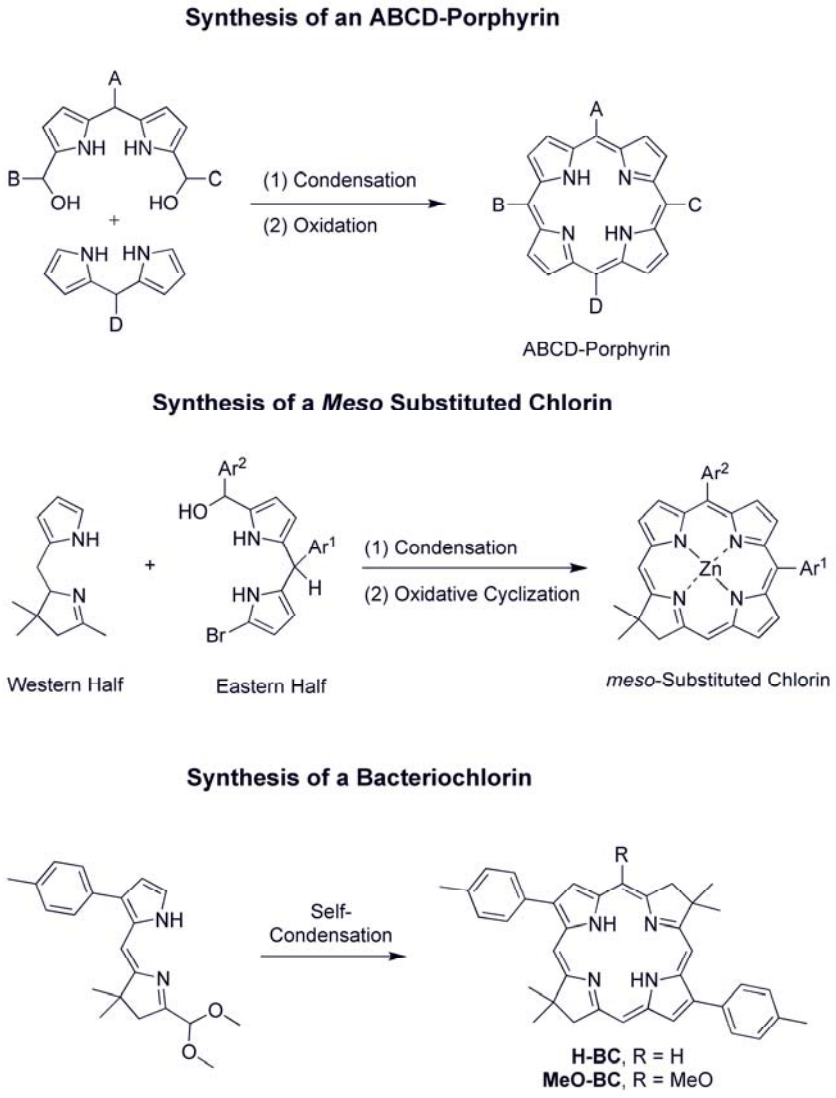

Chart I.4. Syntheses of a porphyrin, chlorin, and bacteriochlorin.

5. Applications. Because of their unique spectral and photophysical properties, porphyrins and hydroporphyrins have been used for biomedical applications,[12] molecular information storage,[13] and solar energy applications.[14] For example, porphyrins have been

used as photosensitizers for photodynamic therapy (PDT), an emerging treatment for cancer.[12] Bacteriochlorins are the best candidates for PDT photosensitizers because the Q_y band is in the near-IR region, followed by chlorins and then porphyrins. Porphyrins are attractive candidates for molecular information storage applications because they can form long-lived cation radicals that can be tuned by varying the substituents on the macrocycle.[13] Additionally, porphyrins have been used for artificial photosynthesis applications due to their resemblance to chlorophylls and bacteriochlorophylls.[14]

I.B. ß-Substituted Chlorins

Chlorophyll *a* and *b* play an important role in plant photosynthesis. The structures of chlorophyll *a* and *b* are shown in Chart I.5. Chlorophyll *a* contains several important features, including a centrally coordinated divalent magnesium, a vinyl group in the 3-position, and an exocyclic five-membered ring containing a 13^1-oxo group. Chlorophyll *b* differs from chlorophyll *a* in that the former contains a formyl group in the 7-position, while the latter contains a methyl group.

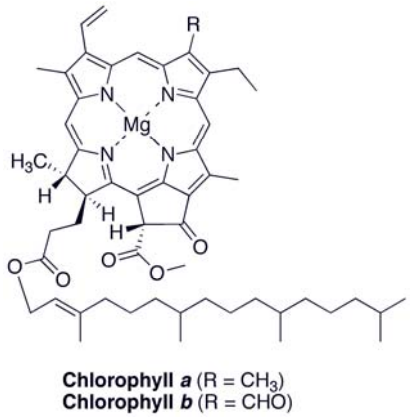

Chlorophyll *a* (R = CH_3)
Chlorophyll *b* (R = CHO)

Chart I.5. Structures of chlorophyll *a* and *b*.

Due to the importance of chlorophyll *a* and *b*, the Lindsey group has synthesized chlorins with electron withdrawing groups in the 3- and 13-positions to determine the effects of electron withdrawing groups on the chlorin macrocycle[15] (Chart I.6). By altering the substituents at the 3- and 13-position, the absorption of the Q_y band can be tuned. Electron withdrawing groups at the 3- and/or 13-position result in a bathochromic shift of both the B and Q_y bands, as well as an increase in the intensity of the Q_y band relative to the B band.[15]

However, not much is currently known about the effects of electron donating groups on the chlorin macrocycle. As a result, the synthesis of chlorins bearing electron donating groups is explored in Chapter II of this thesis.

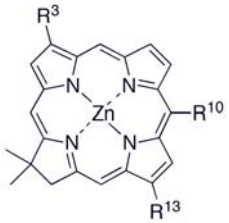

Chart I.6. Diagram indicating the 3-, 10-, and 13-positions on the chlorin macrocycle.

I.C. Carotenoid-Porphyrin Dyads

Chlorophyll and bacteriochlorophyll play an important role in photosynthetic systems, absorbing light and forming the basis of antenna complexes known as light-harvesting arrays. Light-harvesting arrays are comprised of hundreds of molecules in elaborate three-dimensional architectures.[16] The light-harvesting arrays funnel energy to the reaction centers.

In addition to pigments such as chlorophylls and bacteriochlorophylls, photosynthetic systems contain carotenoids.[2] Carotenoids are pigments consisting of a large conjugated π system that perform several important functions in photosynthetic systems, including light harvesting, photoprotection, and the dissipation of excess energy.[2] As a result of the important functions carotenoids play in photosynthesis, a significant number of carotenoid-porphyrin dyads have been synthesized as models for light-harvesting arrays.[17-25] These dyads have been synthesized previously by modifying *trans*-ß-apo-8′-carotenal or another carotenoid to produce a compound that could be linked to the porphyrin via an amide,[20] ester,[22] or ether[22] linkage. Additionally, these dyads have been synthesized by using a carotenoid-linked aryl aldehyde during acid-catalyzed porphyrin formation.[25]

The Lindsey group recently developed a new method of synthesizing chalcone derivatives of hydroporphyrins by reaction of an aldehyde (including enals) and an acetyl-substituted chlorin or bacteriochlorin.[26] Chapter III of this thesis will focus on the facile synthesis and characterization of carotenoid-porphyrin dyads using an acetyl porphyrin and the commercially available *trans*-β-apo-8′-carotenal.

I.D. Overview

Chapter II will focus on the synthesis of chlorins with electron donating groups in the 3-position. Currently, there is very little known about the effects of electron donating groups on the chlorin because most of the work to date has focused on electron withdrawing groups.[15] The facile synthesis of carotenoid-porphyrin dyads for artificial photosynthesis will be discussed in Chapter III. Carotenoid-porphyrin dyads have been synthesized previously, but the majority of these syntheses required modification of *trans*-ß-apo-8′-carotenal or another carotenoid to produce a species that could be linked to the porphyrin,[23] whereas the synthesis described in Chapter III requires no modification of *trans*-ß-apo-8′-carotenal.

I.E. References

(1) Milgrom, L. R. *Colours of Life*; Oxford University Press: New York, 1997; Chapter 1.

(2) Blankenship, R. E. *Molecular Mechanisms of Photosynthesis*. Blackwell Science: Oxford, 2002; Chapter 4.

(3) Wilks, A. In *Heme, Chlorophyll, and Bilins: Methods and Protocols*; Smith, A. G.; Witty, M., Eds.; Humana Press Inc., Totowa, New Jersey, 2002; pp 157–184.

(4) Milgrom, L. R. *Colours of Life*; Oxford University Press: New York, 1997; Chapter 2.

(5) Pavlov, V. Y.; Ponomarev, G. V. *Chem. Heterocycl. Compd.* **2004**, *40*, 393–425.

(6) Sasaki, S.-I.; Tamiaki, H. *J. Org. Chem.* **2006**, *71*, 2648−2654.

(7) Sasaki, S.-I.; Mizoguchi, T.; Tamiaki, H. *J. Org. Chem.* **2007**, *72*, 4566−4569.

(8) Macpherson, A. N.; Liddell, P. A.; Kuciauskas, D.; Tatman, D.; Gillbro, T.; Gust, D.; Moore, T. A.; Moore, A. L. *J. Phys. Chem. B* **2002**, *106*, 9424−9433.

(9) Zaidi, S. H. H.; Fico, R. M.; Lindsey, J. S. *Org. Process Res. Dev.* **2006**, *10*, 118–134.

(10) Taniguchi, M.; Ra, D.; Mo, G.; Balasubramanian, T.; Lindsey, J. S. *J. Org. Chem.* **2001**, *66*, 7342−7354.

(11) Kim, H.-J.; Lindsey, J. S. *J. Org. Chem.* **2005**, *70*, 5475–5486.

(12) Nyman, E. S.; Hynninen, P. H. *J. Photochem. Photobiol. B* **2004**, *73*, 1–28.

(13) Liu, Z. M.; Yasseri, A. A.; Lindsey, J. S.; Bocian, D. F. *Science* **2003**, *302*, 1543–1545.

(14) Guldi, D. M. *Chem. Soc. Rev.* **2002**, *31*, 22–36.

(15) Laha, J. K.; Muthiah, C.; Taniguchi, M.; McDowell, B. E.; Ptaszek, M.; Lindsey, J. S. *J. Org. Chem.* **2006**, *71*, 4092–4102.

(16) Blankenship, R. E. *Molecular Mechanisms of Photosynthesis.* Blackwell Science: Oxford, 2002; Chapter 5.

(17) Gust, D; Moore, T. A.; Moore, A. L.; Devadoss, C.; Liddell, P. A.; Hermant, R.; Nieman, R. A.; Demanche, L. J.; DeGraziano, J. M.; Gouni, I. *J. Am. Chem. Soc.* **1992**, *114*, 3590–3603.

(18) Bensasson, R. V.; Land, E. J.; Moore, A. L.; Crouch, R. L.; Dirks, G.; Moore, T. A.; Gust, D. *Nature* **1981**, *290*, 329–332.

(19) (a) Effenberger, F.; Schlosser, H.; Bäuerle, P.; Maier, S.; Port, H; Wolf, H. C. *Angew. Chem. Int. Ed. Engl.* **1988**, *26*, 281–284. (b) Momenteau, M.; Loock, B.; Seta, P.; Bienvenue, E.; d'Epenoux, B. *Tetrahedron* **1989**, *45*, 4893–4901.

(20) Hermant, R. M.; Liddell, P. A.; Lin, S.; Alden, R. G.; Kang, H. K.; Moore, A. L.; Moore, T. A.; Gust, D. *J. Am. Chem. Soc.* **1993**, *115*, 2080–2081.

(21) Tatman, D.; Liddell, P. A.; Moore, T. A.; Gust, D.; Moore, A. L. *Photochem. Photobiol.* **1998**, *68*, 459–466.

(22) Gust, D.; Moore, T. A.; Bensasson, R. V.; Mathis, P.; Land, E. J.; Chachaty, C.; Moore, A. L.; Liddell, P. A.; Nemeth, G. A. *J. Am. Chem. Soc.* **1985**, *107*, 3631–3640.

(23) Gust, D.; Moore, T. A.; Moore, A. L.; Liddell, P. A. *Methods Enzymol.* **1992**, *213*, 87–100.

(24) Fungo, F.; Otero, L.; Durantini, E.; Thompson, W. J.; Silber, J. J.; Moore, T. A.; Moore, A. L.; Gust, D.; Sereno, L. *Phys. Chem. Chem. Phys.* **2003**, *5*, 469–475.

(25) Osuka, A.; Yamada, H.; Maruyama, K. *Chem. Lett.* **1990**, 1905–1908.

(26) Ruzié , C.; Krayer, M.; Lindsey, J. S. *Org. Lett.* **2009**, *11*, 1761–1764.

II. Chlorins Bearing an Electron Donating Group in the 3-Position

II.A. Introduction

Chlorins are a type of hydroporphyrin that differ from porphyrins owing to the presence of a reduced pyrrole ring in the macrocycle. One of the most recognizable naturally occurring chlorins is chlorophyll *a*, which is central to plant photosynthesis. Synthetic chlorins with varying groups on the 3- and 13-positions are desirable targets due to their similarity to chlorophyll *a*, which has a vinyl group in the 3-position and a keto-group in the 13-position (Chart II.1).

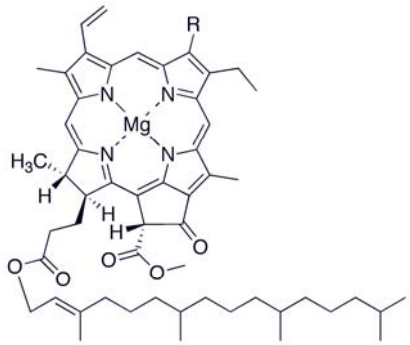

Chlorophyll *a* (R = CH_3)
Chlorophyll *b* (R = CHO)

Chart II.1. Structures of chlorophyll *a* and *b*.

As a result, the Lindsey group has synthesized chlorins with electron withdrawing groups in the 3- and 13-positions (Chart II.2).[1] Electron withdrawing groups at the 3- and/or 13-position result in a bathochromic shift of both the B and Q_y bands, as well as an increase in the intensity of the Q_y band relative to the B band.[1] The absorption of the Q_y band can be

tuned by changing the groups at the 3- and 13-positions (Figure II.1). The 3- and 13-positions are both in a pyrrole ring that lies along the Q_y axis, with the 3-position distal and 13-position proximal to the pyrroline ring (Chart II.3). Currently, not much is known about the effects of electron donating groups on the chlorin. Therefore, we would like to synthesize chlorins bearing (1) electron donating groups in the 3-position, (2) electron donating groups in both the 3- and 13-positions, (3) an electron donating group in the 3-position and an isocyclic ring containing a 13-keto group, and (4) an electron donating group in the 3-position and an electron withdrawing group in the 13-position (push-pull chlorins).

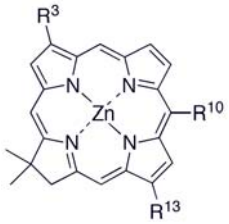

Chart II.2. Diagram indicating the 3-, 10-, and 13-positions on the chlorin macrocycle.

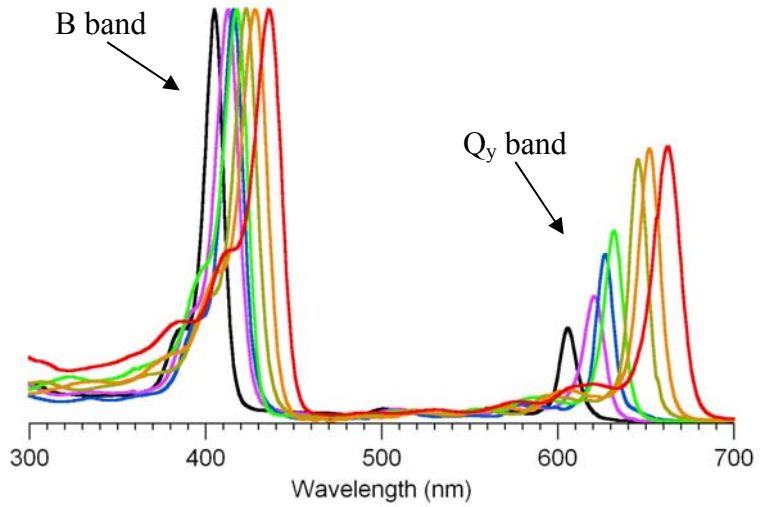

Figure II.1. Absorption spectra in toluene at room temperature of 3,13-substituted chlorins: H,H, (black); V,H (violet); E,H (blue); H,A (green); E,E (gold); E,A (orange); A,A (red).[1] Key: A = acetyl, Br = bromo, E = TIPS-ethynyl, F = formyl, H = hydrogen, Ph = phenyl, P = phenylethynyl, V = vinyl. Spectra are normalized at the B band.

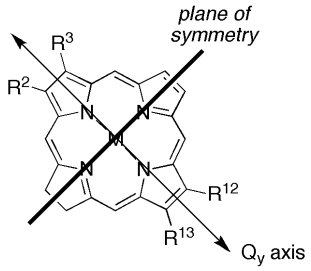

Chart II.3. Diagram illustrating the Q_y axis in the chlorin.

Push-pull chlorins may have applications in the fields of optics and molecular-based information storage.[2] Push-pull porphyrins have been made previously (Chart II.4), and some have exhibited large bathochromic shifts in both the B- and Q-transitions, increased extinction coefficients, and broadened absorption bands relative to the parent porphyrin.[2,3]

For example, adding push and pull groups to the porphyrin causes a bathochromic shift of λ_B by 42 nm and λ_{Qy} by 146 nm, and the I_B/I_{Qy} ratio changed from 6 (standard) to 2.1 (push-pull).[2,4] Additionally, the optical properties of the push-pull chlorins could be altered by changing the metal center, the electron donating and withdrawing groups, and other substituents on the macrocycle.

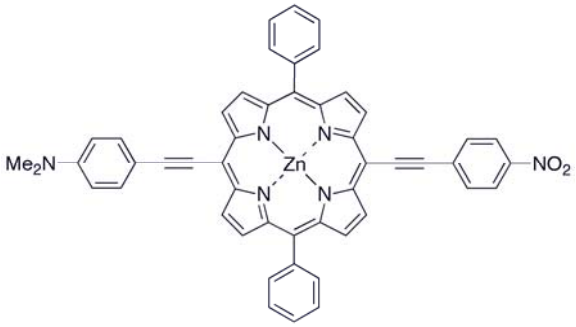

Chart II.4. Example of a push-pull porphyrin.

This chapter discusses the syntheses of three chlorins with electron donating groups in the 3-position, **ZnC-SMe^{3}M^{10}**, **ZnC-OMe^{3}M^{10}**, and **ZnC-(NMe$_2$)^{3}M^{10}**. The structures of these compounds are shown in Chart II.5.

Chart II.5. Structures of **ZnC-SMe^{3}M^{10}**, **ZnC-OMe^{3}M^{10}**, and **ZnC-(NMe$_2$)^{3}M^{10}**.

II.B. Results and Discussion

1. Synthesis. a. Chlorin Formation. The 3-bromochlorin **ZnC-Br^{3}M^{10}** was formed by condensing compound **1** (western half)[1] and compound **2** (eastern half)[1] in CH_2Cl_2 containing methanolic *p*-TsOH·H_2O under argon as shown in Scheme II.1. The reddish-brown mixture was neutralized with 2,2,6,6-tetramethylpiperidine, concentrated, and treated with $Zn(OAc)_2$ and AgOTf in CH_3CN at reflux exposed to air for 14 h. Following column chromatography, the 3-bromochlorin **ZnC-Br^{3}M^{10}** was obtained in 34% yield.

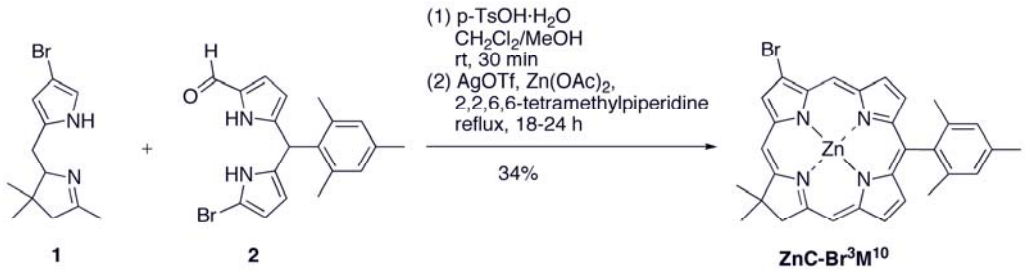

Scheme II.1. Synthesis of **ZnC-Br^{3}M^{10}**.

b. Chlorin Derivatization. The syntheses of 3-methylthiochlorin **ZnC-SMe^{3}M^{10}** and 3-methoxychlorin **ZnC-OMe^{3}M^{10}** are shown in Scheme II.2. Palladium coupling of **ZnC-Br^{3}M^{10}** with sodium thiomethoxide was carried out under conditions used for aryl thioether formation (20 mol% of $Pd_2(dba)_3$ and Xantphos in refluxing xylene),[5] affording 3-methylthiochlorin **ZnC-SMe^{3}M^{10}** in 95% yield. Similarly, palladium coupling of **ZnC-**

Br^{3}M^{10} with sodium methoxide in the presence of 20 mol% of $Pd_2(dba)_3$ and Xantphos in refluxing xylene gave 3-methoxychlorin **ZnC-OMe^{3}M^{10}** in 16% yield.

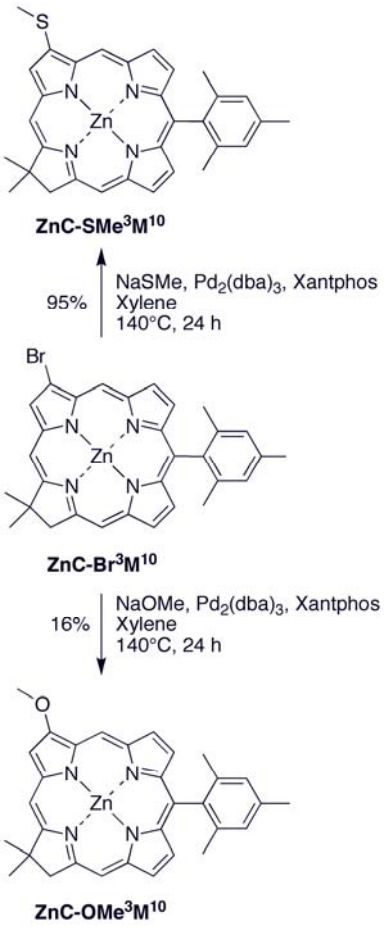

Scheme II.2. Chlorin derivatization to form **ZnC-SMe^{3}M^{10}** and **ZnC-OMe^{3}M^{10}**.

As a result of the low yield for the 3-methoxychlorin, further attempts at synthesizing **ZnC-OMe^{3}M^{10}** were made. The first strategy focused on installing the methoxy group on the western half prior to chlorin formation as shown in Scheme II.3.

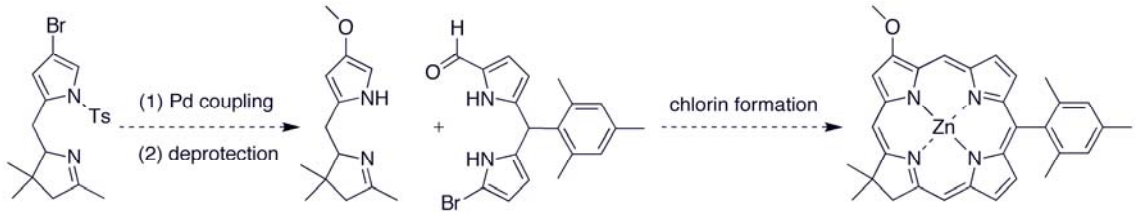

Scheme II.3. Strategy for installation of the methoxy group on the western half (prior to chlorin formation).

Schemes II.4 and II.5 show the attempted synthesis of the tosyl-protected, methoxy-substituted western half **4**. Following a procedure for the copper-catalyzed reaction of sodium methoxide with aryl bromides,[6] **3** was reacted with sodium methoxide (10 equiv) and CuBr (1 equiv) in methanol for 24 h at 65 °C (Scheme II.4). However, no product was formed. Therefore, a modification was made whereby **3** was reacted with sodium methoxide (3 equiv), CuBr (1 equiv), and $Pd_2(dba)_3$ (30 mol%) in refluxing xylene for 24 h (Scheme II.5). This also did not result in product formation.

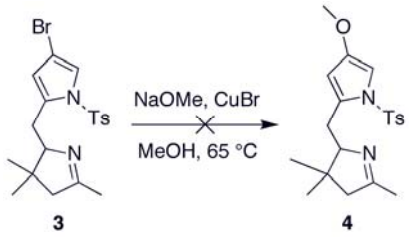

Scheme II.4. Attempted synthesis of the tosyl-protected, methoxy-substituted western half **4** using a copper catalyst.

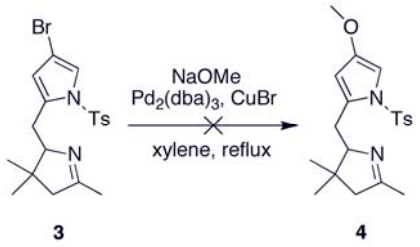

Scheme II.5. Attempted synthesis of the tosyl-protected, methoxy-substituted western half **4** using copper and palladium catalysts.

An additional attempt at forming a methoxy-substituted chlorin is shown in Scheme II.6. Following a modification of a method for installing a methoxy group on the *meso* position of a porphyrin,[7] palladium coupling of **ZnC-Br^{3}M^{10}** with methanol (4 equiv) using 20 mol% of $Pd_2(dba)_3$ and Xantphos with Cs_2CO_3 (2 equiv) in toluene at 110 °C for 24 h was attempted. However, this method did not yield any of the desired product.

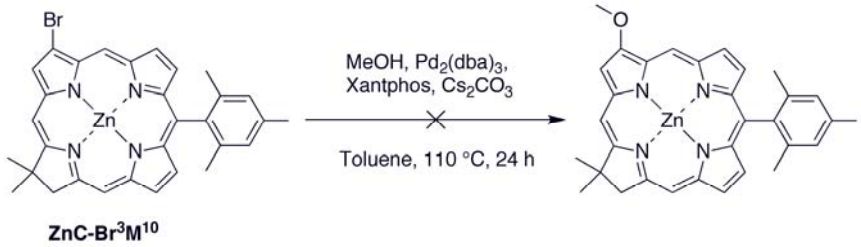

Scheme II.6. Attempted synthesis of a 3-methoxy-substituted chlorin.

The synthesis of 3-dimethylaminochlorin **ZnC-(NMe$_2$)^{3}M^{10}** is shown in Scheme II.7. Palladium coupling of **ZnC-Br^{3}M^{10}** with dimethylamine (10 equiv) was carried out using $Pd(OAc)_2$ (40 mol%), (*t*-Bu)$_3$PHBF$_4$ (40 mol%), and NaO*t*-Bu (3 equiv) in refluxing toluene for 48 h,[8] affording 3-dimethylaminochlorin **ZnC-(NMe$_2$)^{3}M^{10}** in 49% yield.

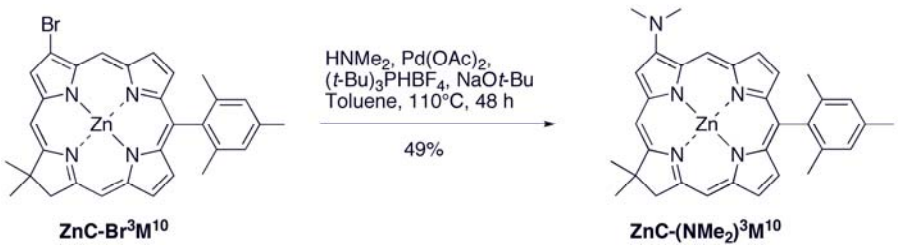

ZnC-Br^{3}M^{10} **ZnC-(NMe$_2$)^{3}M^{10}**

Scheme II.7. Synthesis of **ZnC-(NMe$_2$)^{3}M^{10}**.

2. Absorption Spectroscopy. The spectral properties of the zinc chlorins are listed in Table II.1, and the absorption spectra are included as Figure II.2. The spectral properties of **ZnC-(NMe$_2$)^{3}M^{10}**, **ZnC-OMe^{3}M^{10}**, and **ZnC-SMe^{3}M^{10}** can be compared with the benchmark zinc chlorin **ZnC-M^{10}**, which lacks a 3-substituent. For **ZnC-(NMe$_2$)^{3}M^{10}**, the B band was at 410 nm and the Q_y band was at 612 nm, resulting in a bathochromic shift relative to the benchmark chlorin **ZnC-M^{10}**. This bathochromic shift is accompanied by an increase in intensity of the Q_y band relative to the B band. For **ZnC-OMe^{3}M^{10}**, the B band was at 404 nm and the Q_y band was at 603 nm, resulting in a hypsochromic shift relative to the benchmark chlorin **ZnC-M^{10}**. This hypsochromic shift is accompanied by a small decrease in the intensity of the Q_y band relative to the B band. For **ZnC-SMe^{3}M^{10}**, the B band was at 410 nm and the Q_y band was at 616 nm, resulting in a bathochromic shift relative to the benchmark chlorin **ZnC-M^{10}**. This bathochromic shift is accompanied by an increase in the intensity of the Q_y band relative to the B band.

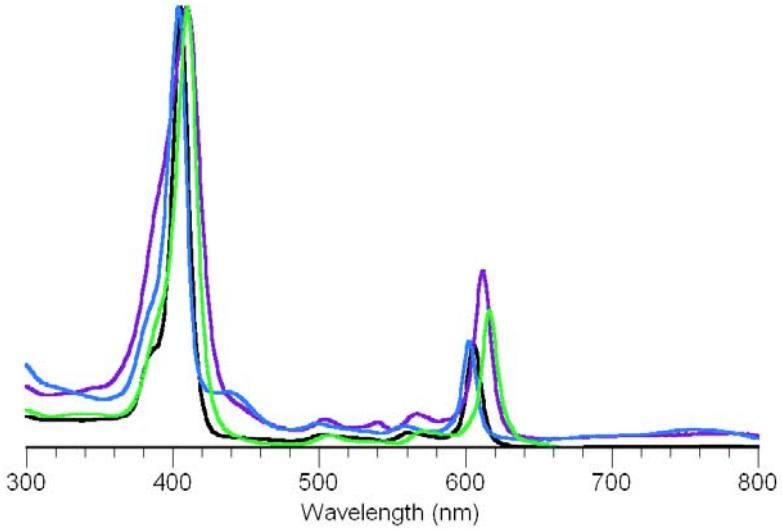

Figure II.2. Absorption spectra in toluene at room temperature of **ZnC-M**^{10}, **ZnC-(NMe$_2$)**^{3}**M**^{10}, **ZnC-OMe**^{3}**M**^{10}, and **ZnC-SMe**^{3}**M**^{10}. Spectra are normalized at the B band.

Table II.1. Absorption spectral properties.[a]

Compound	λ_B (nm)	$\Delta\nu_B$ (cm^{-1})	λ_{Qy} (nm)	$\Delta\nu_{Qy}$ (cm^{-1})	I_B/I_Q
ZnC-M^{10}	405	0	606	0	4.2
ZnC-(NMe$_2$)^3**M**^{10}	410	301	612	162	2.5
ZnC-OMe^3**M**^{10}	404	-61	603	-82	4.3
ZnC-SMe^3**M**^{10}	410	301	616	268	3.0

[a] In toluene at room temperature, normalized at the B band.

3. Emission Spectroscopy. The chlorins were analyzed by fluorescence emission spectroscopy. All spectra were obtained in toluene at room temperature. The absorption of the B band was set to approximately 0.1, and all chlorins were excited at the wavelength of

the B band. The fluorescence emission spectra are typical of chlorins, with a stronger Q(0,0) band and weaker Q(0,1) band. The fluorescence emission spectra for the chlorins bearing electron donating groups is in Figure II.3, and the emission properties are listed in Table II.2.

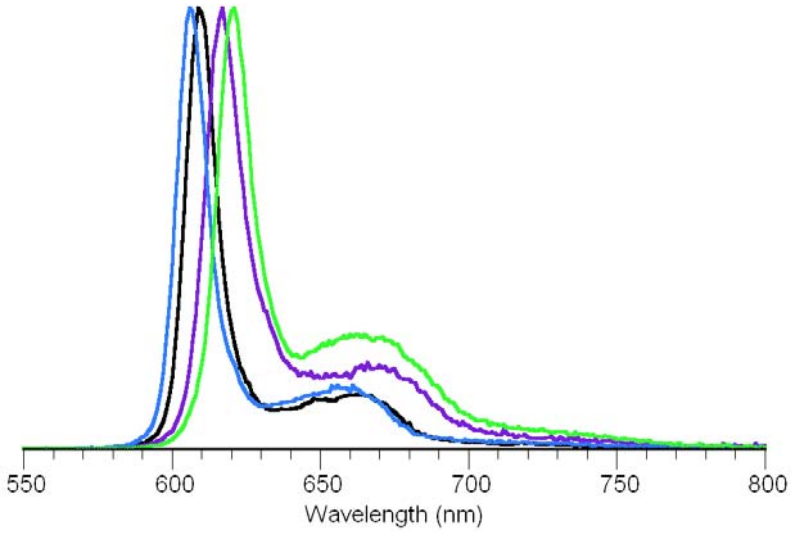

Figure II.3. Emission spectra in toluene at room temperature of **ZnC-M**[10], **ZnC-(NMe$_2$)**^{3}**M**[10], **ZnC-OMe**^{3}**M**[10], and **ZnC-SMe**^{3}**M**[10]. Spectra are normalized at the Q(0,0) band.

Table II.2. Emission spectral properties.[a]

Compound	λ_{em} (nm) Q(0,0)	λ_{em} (nm) Q(0,1)
ZnC-M[10]	609	665
ZnC-(NMe$_2$)^3**M**[10]	617	664
ZnC-OMe^3**M**[10]	606	656
ZnC-SMe^3**M**[10]	621	666

[a] In toluene at room temperature.

II.C. Conclusion

The initial target chlorins featuring electron donating groups in the 3-position were synthesized. For **ZnC-(NMe$_2$)^{3}M^{10}** and **ZnC-SMe^{3}M^{10}**, the B band and the Q_y band were bathochromically shifted relative to the benchmark chlorin **ZnC-M^{10}**, and the intensity of the Q_y band increased relative to the B band. However, for **ZnC-OMe^{3}M^{10}**, the B band and the Q_y band were hypsochromically shifted relative to the benchmark chlorin **ZnC-M^{10}**, and the intensity of the Q_y band decreased relative to the B band. Therefore, the effects of electron donating groups on the chlorin macrocycle are not as clear as for electron withdrawing groups, which produce a bathochromic shift of the B and Q_y bands and an increase in the intensity of the Q_y band relative to the B band. A method for installing the electron donating groups on the western half prior to chlorin formation will be necessary to synthesize a push-pull chlorin. This work lays the foundation for the future synthesis of push-pull chlorins.

II.D. Experimental Section

General Methods. ^{1}H NMR (300 MHz) spectra were collected at room temperature in $CDCl_3$. Absorption spectra were obtained in toluene at room temperature. All samples were analyzed by laser desorption mass spectrometry (LD-MS) using 1,4-bis-(5-phenyloxazol-2-yl)benzene (POPOP) as the matrix. Electrospray ionization mass spectroscopy (ESI-MS) data are reported for the molecule ion or protonated molecule ion. Silica gel (40 μm average particle size) was used for column chromatography. THF was freshly distilled from sodium/benzophenone ketyl. Anhydrous toluene, methanol, and xylene

were reagent grade and were used as received.

Non-commercial compounds. The following compounds were synthesized as described in the literature: **1** and **2**.[1]

Zn(II)-3-Bromo-17,18-dihydro-10-mesityl-18,18-dimethylporphyrin (ZnC-Br^{3}M^{10}). Following a streamlined procedure,[9] a solution of **1** (153 mg, 0.569 mmol) and **2** (210 mg, 0.569 mmol) in distilled CH_2Cl_2 was treated with a solution of *p*-TsOH·H_2O (540.9 mg, 2.85 mmol) in anhydrous methanol (6 mL) under argon. The resulting red reaction mixture was stirred at room temperature for 40 min. A sample of 2,2,6,6-tetramethylpiperidine (1.2 mL, 7.11 mmol) was added. The reaction mixture was concentrated. The resulting solid was dissolved in CH_3CN (56.9 mL) and subsequently treated with 2,2,6,6-tetramethylpiperidine (2.4 mL, 14.2 mmol), $Zn(OAc)_2$ (1.62 g, 8.81 mmol), and AgOTf (446 mg, 1.74 mmol). The resulting suspension was refluxed for 14 h exposed to air. The crude mixture was filtered through a pad of silica (CH_2Cl_2). The filtrate was chromatographed [silica, hexanes/CH_2Cl_2 (2:1→1:1→1:2)] to afford a green solid (119 mg, 34%): ^{1}H NMR δ 1.84 (s, 6H), 2.01 (s, 6H), 2.59 (s, 3H), 4.50 (s, 2H), 7.22 (s, 2H), 8.30 (d, *J* = 3.4 Hz, 1H), 8.49 (s, 1H), 8.53 (d, *J* = 3.9 Hz, 1H), 8.60 (d, *J* = 4.5 Hz, 1H), 8.67 (s, 1H), 8.78 (s, 1H), 8.87 (d, *J* = 3.9 Hz, 1H), 9.73 (s, 1H); LD-MS obsd 599.8; ESI-MS obsd 598.0710 [M^{+}], calcd 598.0711 ($C_{31}H_{27}BrN_4Zn$); λ_{abs} 410, 614 nm; λ_{em} (λ_{ex}=410 nm) 617, 647 nm.

Zn(II)-17,18-Dihydro-10-mesityl-18,18-dimethyl-3-methylthioporphyrin (ZnC-SMe^{3}M^{10}). Following a procedure for aryl thioether formation,[5] a mixture of **ZnC-Br^{3}M^{10}**

(45.1 mg, 0.0750 mmol), $Pd_2(dba)_3$ (13.7 mg, 0.0150 mmol, 20 mol %), Xantphos (8.7 mg, 0.0150 mmol, 20 mol %), and sodium thiomethoxide (15.8 mg, 0.225 mmol, 3 equivalents relative to **ZnC-Br^{3}M^{10}**) was dried in a Schlenk flask for 1 h. Degassed xylene (1.5 mL) was added, and the mixture was purged with argon. The reaction mixture was heated to reflux for 24 h. After cooling to room temperature, the reaction mixture was treated with CH_2Cl_2 and water. The organic layer was separated, dried (Na_2SO_4), and concentrated. The resulting residue was chromatographed (silica, CH_2Cl_2) to give a green solid (40.5 mg, 95%): ^{1}H NMR δ 1.86 (s, 6H), 2.02 (s, 6H), 2.59 (s, 3H), 2.80 (s, 3H), 4.47 (s, 2H), 7.21 (s, 2H), 7.72 (s, 1H), 8.19 (d, J = 3.9 Hz, 1H), 8.32 (s, 1H), 8.38 (s, 1H), 8.49 (d, J = 4.5 Hz, 1H), 8.52 (d, J = 4.5 Hz, 1H), 8.59 (s, 1H), 8.74 (d, J = 4.5 Hz, 1H), 9.38 (s, 1H); LDMS obsd 566.5; ESI-MS obsd *m/z* 566.1472 [M^+], calcd 566.1477 ($C_{32}H_{30}N_4SZn$); λ_{abs} 410, 616 nm; λ_{em} (λ_{ex}=410 nm) 621, 666 nm.

Zn(II)-17,18-Dihydro-10-mesityl-3-methoxy-18,18-dimethylporphyrin (ZnC-OMe^{3}M^{10}). Modifying the procedure used to synthesize **ZnC-SMe^{3}M^{10}**,[5] a mixture of **ZnC-Br^{3}M^{10}** (10.0 mg, 0.017 mmol), $Pd_2(dba)_3$ (3.1 mg, 0.0034 mmol, 20 mol %), Xantphos (2.1 mg, 0.0041 mmol, 20 mol %), and sodium methoxide (2.7 mg, 0.051 mmol) was dried in a Schlenk flask for 1 h. Degassed xylene (1.6 mL) was added, and the mixture was purged with argon. The reaction mixture was heated to reflux for 24 h. After cooling to room temperature, the reaction mixture was treated with CH_2Cl_2 and water. The organic layer was separated, dried (Na_2SO_4), and concentrated. The resulting residue was chromatographed [silica, hexanes/CH_2Cl_2 (1:1→1:2)] to give a green solid (1.5 mg, 16%): ^{1}H NMR δ 1.85 (s,

6H), 1.98 (s, 6H), 2.58 (s, 3H), 4.41 (s, 2H), 7.19 (s, 2H), 7.74 (s, 1H), 8.26 (d, J = 3.9 Hz, 1H), 8.29 (s, 1H), 8.44 (d, J = 3.9 Hz, 1H), 8.46 (d, J = 3.9 Hz, 1H), 8.50 (s, 1H), 8.66 (d, J = 3.9 Hz, 1H), 9.51 (s, 1H); LDMS obsd 551.0; ESI-MS obsd 550.1707 [M^+], calcd 550.1706 ($C_{33}H_{28}N_4OZn$); λ_{abs} 404, 603 nm; λ_{em} (λ_{ex} = 410 nm) 606, 656 nm.

Zn(II)-17,18-Dihydro-3-dimethylamino-10-mesityl-18,18-dimethylporphyrin (ZnC-(NMe$_2$)^{3}M^{10}). Following a procedure for amination of aryl bromides[8] with a slight modification, a mixture of **ZnC-Br^{3}M^{10}** (10.0 mg, 0.017 mmol), $Pd(OAc)_2$ (1.5 mg, 0.0068 mmol, 40 mol %), (t-Bu)$_3$PHBF$_4$ (1.9 mg, 0.0068 mmol, 40 mol %), and sodium t-butoxide (4.9 mg, 0.051 mmol, 3 equiv) were dried in a Schlenk flask for 1 h. Degassed toluene (1.6 mL) and dimethylamine (85 μL, 2.0 M in toluene, 0.17 mmol, 10 equiv) were added, and the mixture was purged with argon. The reaction mixture was heated to reflux for 48 h. After cooling to room temperature, the reaction mixture was treated with CH_2Cl_2 and water. The organic layer was separated, dried (Na_2SO_4), and concentrated. The resulting residue was chromatographed [silica, hexanes/CH_2Cl_2 (1:1→1:2)], followed by a second column (silica, CH_2Cl_2 with 1% TEA) to give a green solid (4.6 mg, 49%, 95% purity): ^{1}H NMR δ 1.87 (s, 6H), 1.95 (s, 6H), 2.58 (s, 3H), 3.61 (s, 6H), 4.36 (s, 2H), 7.19 (s, 2H), 7.69 (s, 1H), 8.18 (s, 1H), 8.22 (d, J = 4.1 Hz, 1H), 8.39 (m, 3H), 8.61 (d, J = 4.1 Hz, 1H), 9.49 (s, 1H); LDMS obsd 563.1; ESI-MS obsd *m/z* 564.2097 $(M + H)^+$ corresponds to 563.2021 (M), calcd 563.2027 ($C_{33}H_{33}N_5Zn$); λ_{abs} 410, 612 nm; λ_{em} (λ_{ex} = 410 nm) 617, 664 nm.

II.E. References

(1) Laha, J. K.; Muthiah, C.; Taniguchi, M.; McDowell, B. E.; Ptaszek, M.; Lindsey, J. S. *J. Org. Chem.* **2006**, *71*, 4092–4102.

(2) Yeung, M.; Ng, A. C. H.; Drew, M. G. B.; Vorpagel, E.; Breitung, E. M.; McMahon, R. J.; Ng, D. K. P. *J. Org. Chem.* **1998**, *63*, 7143–7150.

(3) Priyardarshy, S.; Therien, M. J.; Beratan, D. N. *J. Am. Chem. Soc.* **1996**, *118*, 1504–1510.

(4) Song, X.-Z.; Jentzen, W.; Jia, S.-L.; Jaquinod, L.; Nurco, D. J.; Medforth, C. J.; Smith, K. M.; Shelnutt, J. A. *J. Am. Chem. Soc.* **1996**, *118*, 12975–12988.

(5) Mispelaere-Canivet, C.; Spindler, J.-F.; Perrio, S.; Beslin, P. *Tetrahedron* **2005**, *61*, 5253–5259.

(6) Aalten, H. L.; van Koten, G.; Grove, D. M.; Kuilman, T.; Piekstra, O. G.; Hulshof, L. A.; Sheldon, R. A. *Tetrahedron* **1989**, *45*, 5565–*5578*.

(7) Gao, G.-Y.; Colvin, A. J.; Chen, Y.; Zhang, X. P. *Org. Lett.* **2003**, *5*, 3261–3264.

(8) Thanh, N.C.; Ikai, M.; Kajioka, T.; Fujikawa, H.; Taga, Y.; Zhang, Y.; Ogawa, S.; Shimada, H.; Miyahara, Y.; Kuroda, S.; Oda, M. *Tetrahedron* **2006**, *62*, 11227–11239.

(9) Muthiah, C.; Ptaszek, M.; Nguyen, T. M.; Flack, K. M.; Lindsey, J. S. *J. Org. Chem.* **2007**, *72*, 7736–7749.

III. Facile Synthesis of Carotenoid-Porphyrin Dyads for Artificial Photosynthesis

III.A. Introduction

Photosynthesis plays a critical role in nature, providing all the food and the majority of energy resources on the planet.[1] The most common type of photosynthesis involves pigments such as chlorophylls and bacteriochlorophylls, which absorb light and form the basis of antenna complexes known as light-harvesting arrays. Light-harvesting arrays consist of hundreds of molecules in elaborate three-dimensional architectures.[2,3] These light-harvesting arrays serve to funnel energy to the reaction centers.[3] A schematic diagram of a light-harvesting antenna system is shown in Figure III.1.

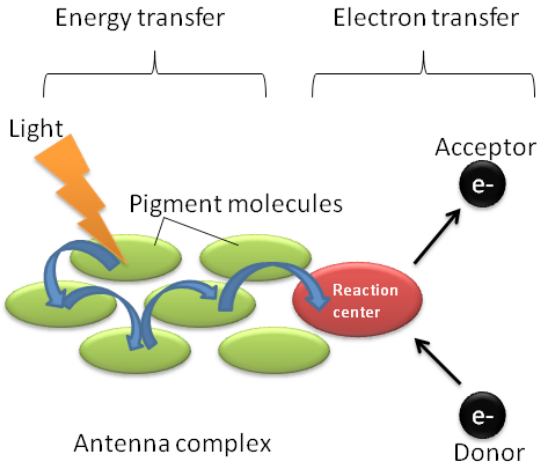

Figure III.1. Schematic diagram of light-harvesting antenna system.

Carotenoids are a class of pigments found in all known photosynthetic organisms,[4] as well as vitamin A and its precursor, β-carotene (Chart III.1). Carotenoids typically consist of a large conjugated π system with a ring structure at the terminal positions.[4] Carotenoids perform several important functions in photosynthetic systems. First, carotenoids assist in the collection of light by absorbing light at wavelengths where chlorophyll weakly absorbs and transferring this energy to chlorophyll.[4,5] Second, carotenoids serve a photoprotective function, quenching triplet states of chlorophyll prior to formation of singlet oxygen.[4] Additionally, they quench singlet oxygen if it forms.[4] Finally, carotenoids regulate energy transfer in antenna complexes by dissipating excess energy as heat in what is known as the xanthophyll cycle.[4,6] This protects the reaction center from overexcitation in the presence of excess light.[6]

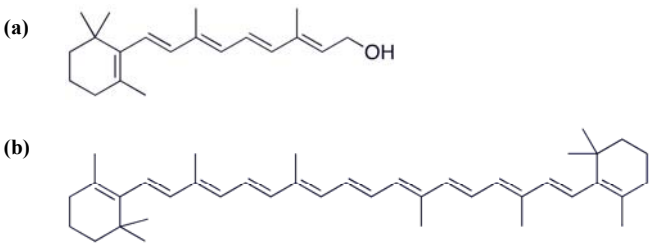

Chart III.1. Structures of (a) vitamin A (retinol) and (b) β-carotene.

As a result of these important functions in photosynthesis, a significant number of carotenoid-porphyrin dyads (carotenoporphyrins) have been synthesized as models for light-harvesting arrays.[5,7-14] Carotenoporphyrins can mimic both the antenna and photoprotective

functions in photosynthesis due to the close interaction of the carotenoid and the π-electron system of the porphyrin.[7] Additionally, some carotenoporphyrins have been designed to produce a charge-separated species.[9] Further, carotenoporphyrins may have applications as diagnostic agents for imaging tumors.[10] Carotenoporphyrins have similar fluorescent properties to porphyrins, but the presence of the carotenoid moiety eliminates phototoxicity.[10]

Carotenoporphyrins have been synthesized previously using amide,[9] ester,[11] and ether[11] linkages (Chart III.2). However, these syntheses all required modification of *trans*-β-apo-8′-carotenal or another carotenoid to produce a species that could be linked to the porphyrin. For example, *trans*-β-apo-8′-carotenal has been used as the starting material to form intermediate carotenoids with ester, carboxylic acid, amine, alcohol, and halogen functionalities (Chart III.3).[12] These intermediates were then connected to the porphyrin in one of three ways: (1) the carotenoid intermediate (ester or carboxylic acid) was converted to an acid chloride derivative and reacted with the porphyrin, (2) the porphyrin was converted to an acid chloride derivative and reacted with the carotenoid (amine or alcohol), or (3) via a Williamson ether synthesis reaction between the carotenoid (halide) and a porphyrin bearing an alcohol group.[12] Additionally, carotenoids of varying lengths have been produced, containing 5-11 conjugated double bonds, using retinal, retinoic acid, and *trans*-β-apo-8′-carotenal as the starting materials (Chart III.4).[13] Carotenoporphyrins have also been synthesized by using a carotenoid-linked aryl aldehyde during acid-catalyzed porphyrin formation (Scheme III.1).[14]

The Lindsey group recently developed a new method of synthesizing chalcone derivatives of hydroporphyrins by reaction of an aldehyde (including enals) and an acetyl-substituted chlorin (Scheme III.2) or bacteriochlorin (Scheme III.3).[15] This chapter will focus on the facile synthesis and characterization of carotenoid-porphyrin dyads using an acetyl porphyrin and the commercially available *trans*-β-apo-8′-carotenal.

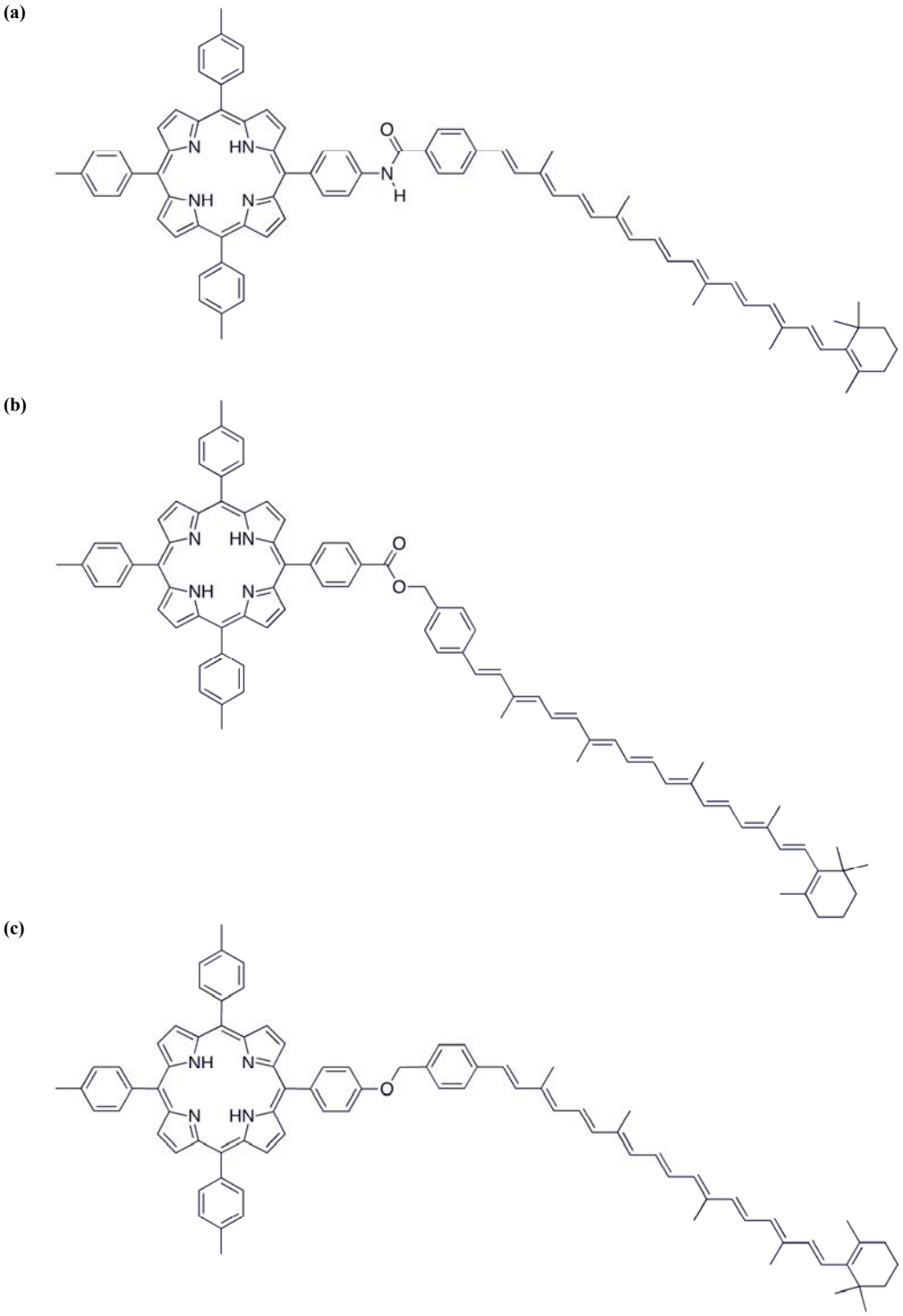

Chart III.2. Examples of carotenoporphyrins connected via (a) amide, (b) ester, and (c) ether linkages.

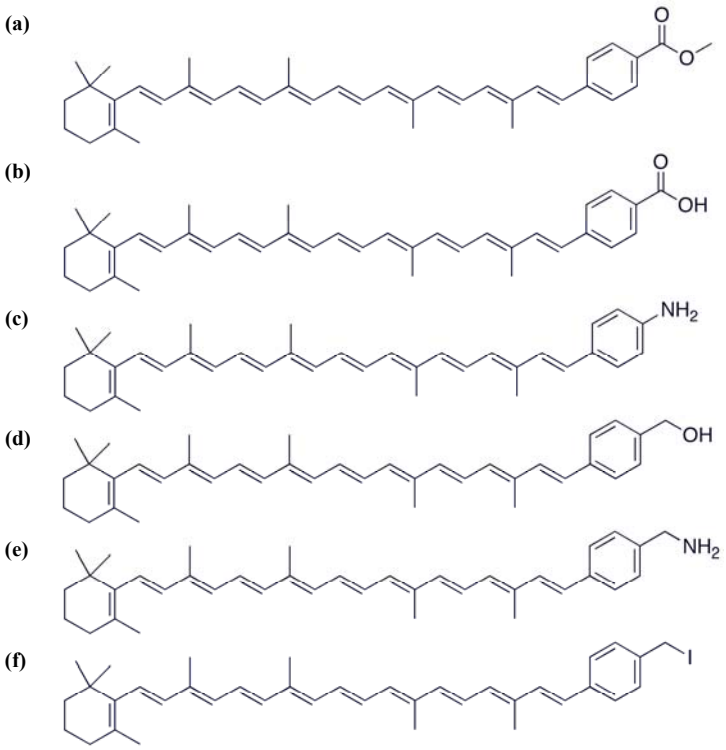

Chart III.3. Examples of intermediate carotenoids bearing ester, carboxylic acid, amine, alcohol, and halogen functionalities that were used to synthesize carotenoporphyrins.[12] The ester and carboxylic acid carotenoids were converted to the acid chloride derivative and then reacted with the porphyrin. The porphyrin was converted to the acid chloride derivative and then reacted with the amine and alcohol carotenoids. The halogen carotenoid was utilized in a Williamson ether synthesis reaction to attach the carotenoid to the porphyrin.

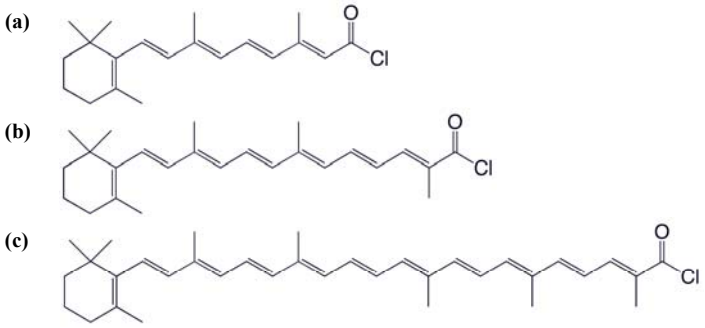

Chart III.4. Examples of carotenoids of varying lengths used to synthesize carotenoporphyrins.[13]

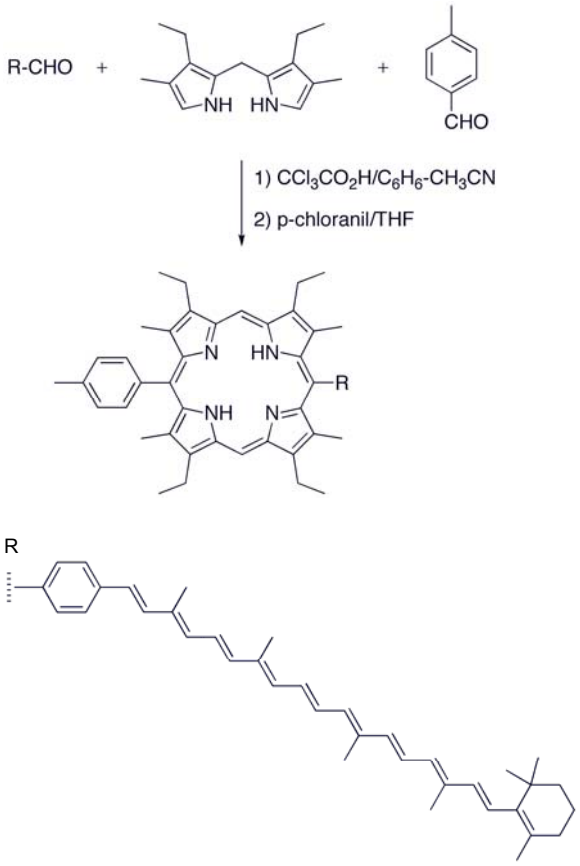

Scheme III.1. Carotenoporphyrin synthesized during acid-catalyzed porphyrin formation.

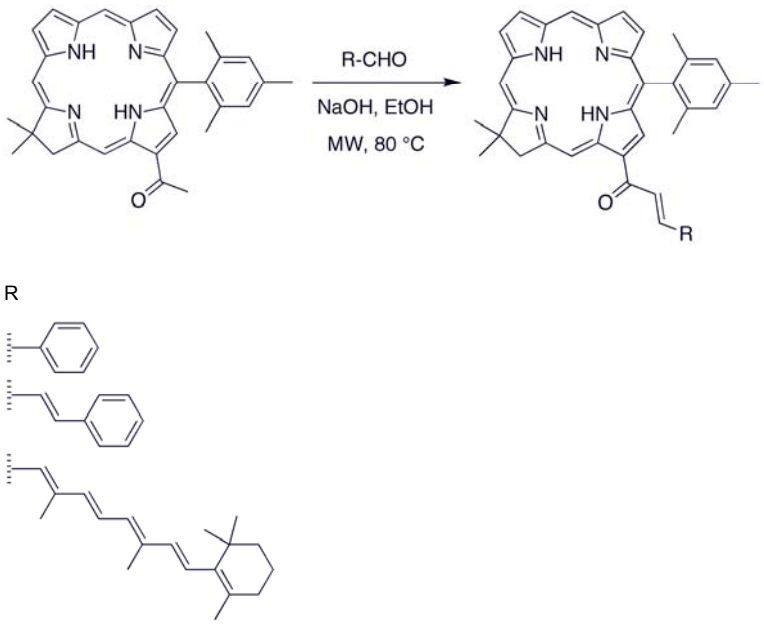

Scheme III.2. Chlorin chalcone derivatives prepared via microwave mediated aldol condensation.

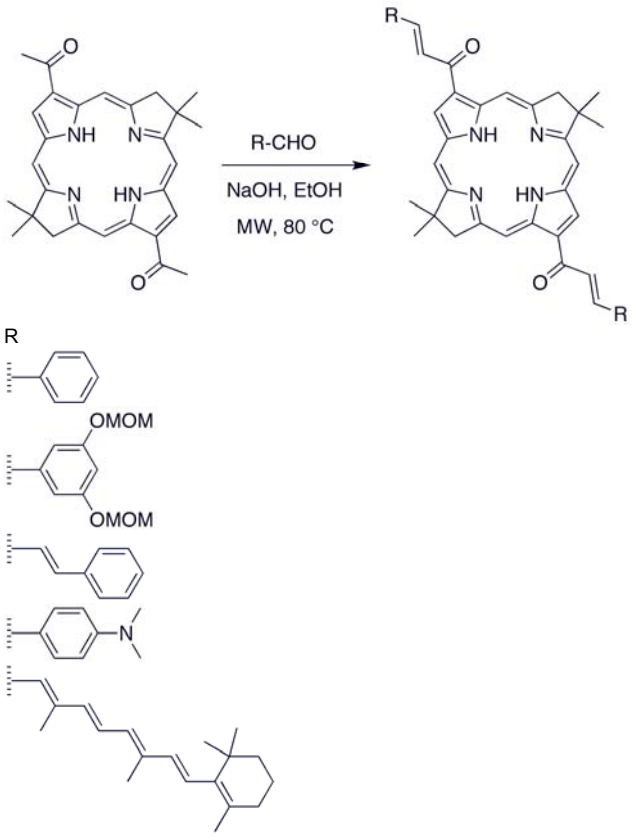

Scheme III.3. Bacteriochlorin chalcone derivatives prepared via microwave mediated aldol condensation.

III.B. Design

The target compounds for this study are shown in Chart III.5. Porphyrins are used in the model system for ease of synthesis when compared to chlorins or bacteriochlorins. The top panel (a) shows a target dyad with aryl groups on three meso positions of the porphryin and the carotenoid moiety directly attached to the porphyrin at the fourth meso position. The middle panel (b) shows a target dyad with the same aryl groups on the three meso positions of the porphyrin, but the carotenoid moiety is separated from the fourth meso position of the

porphyrin by a phenyl linker. A benchmark compound for an aryl substituted carotenoid is shown in the bottom panel (c), which is the result of the aldol condensation of acetophenone and *trans*-β-apo-8′-carotenal.

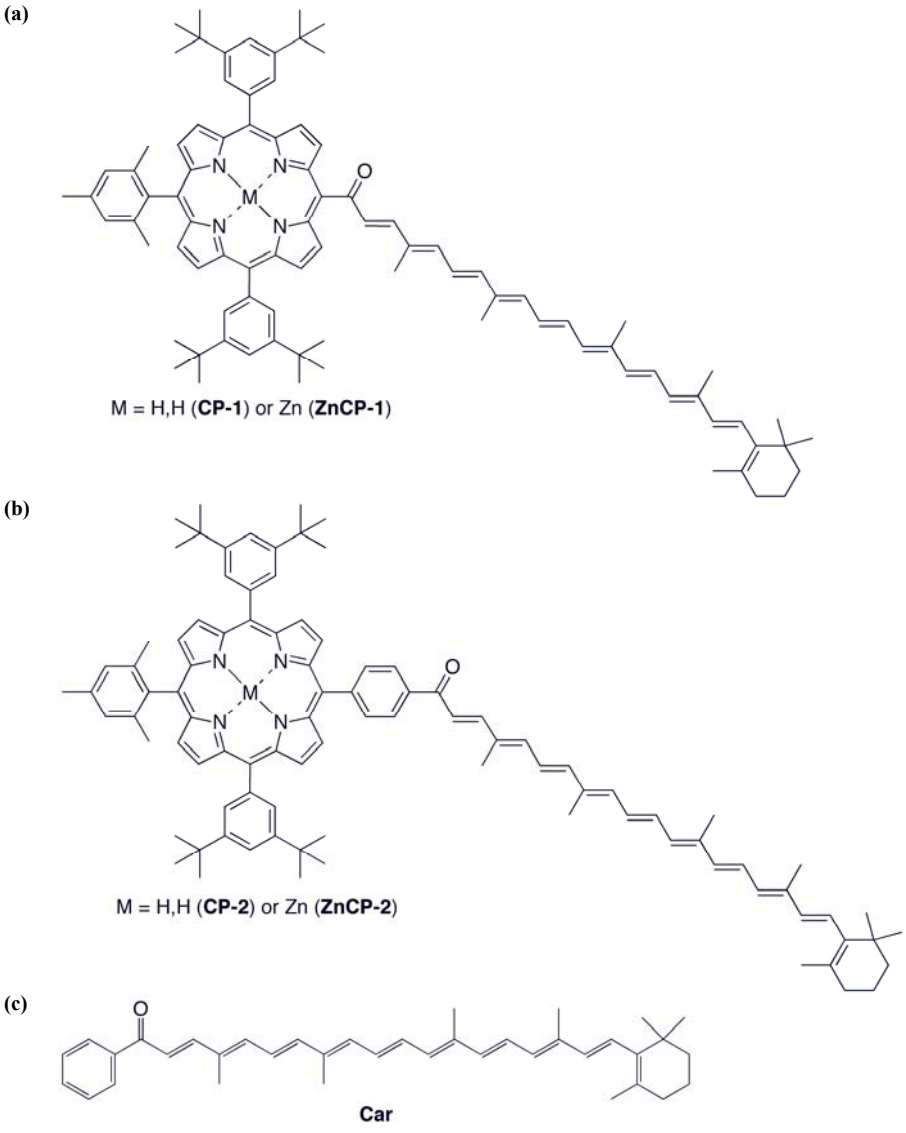

Chart III.5. Target compounds.

III.C. Results and Discussion

1. Synthesis. a. Benchmark Carotenoid. The synthesis of **Car** is shown in Scheme III.4. The aldol condensation under microwave irradiation of acetophenone and *trans*-β-apo-8′-carotenal in the presence of NaOH (10 equiv) in absolute ethanol at 80 °C for

80 minutes afforded **Car** in 59% yield (38.5 mg). **Car** contains a total of ten conjugated carbon-carbon double bonds, whereas *trans*-β-apo-8′-carotenal contains nine.

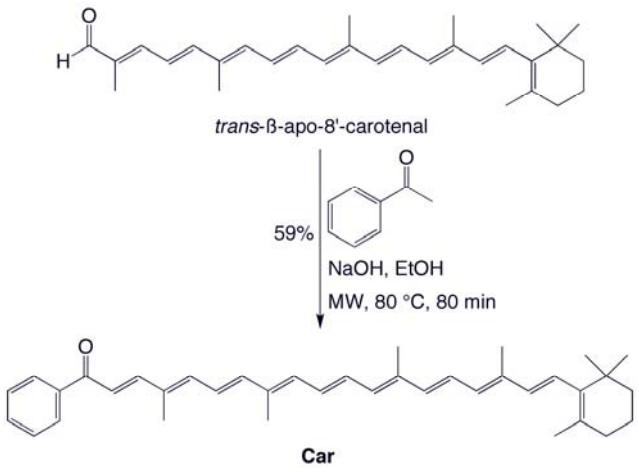

Scheme III.4. Synthesis of **Car**.

b. Benchmark Porphyrins. The syntheses of **P-1** and **ZnP-1** are shown in Scheme III.5. The starting material 5,15-bis(3,5-di-*tert*-butylphenyl)-10-iodo-20-mesitylporphyrin[16] was subjected to Stille coupling with tributyl(1-ethoxyvinyl)tin in the presence of 20 mol% of $(PPh_3)_2PdCl_2$ in THF for 18 hours. Hydrolysis of the intermediate with 10% aqueous HCl gave the acetyl porphyrin **P-1** in 63% yield. Metalation of **P-1** with $Zn(OAc)_2{\cdot}2H_2O$ gave porphyrin **ZnP-1** in 90% yield.

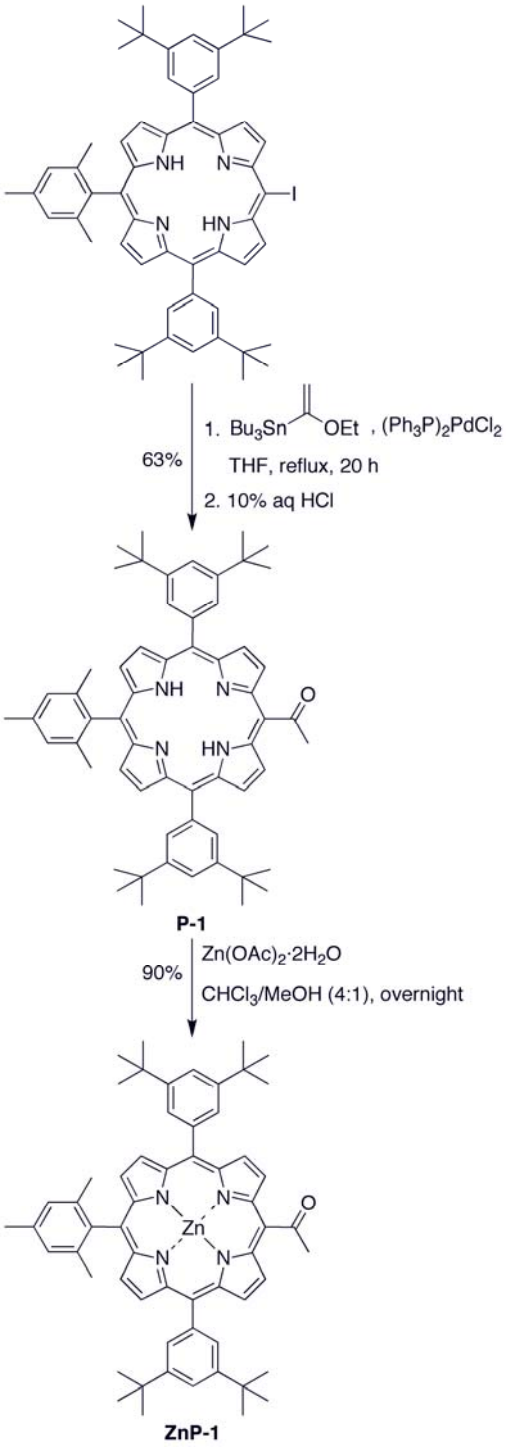

Scheme III.5. Syntheses of **P-1** and **ZnP-1**.

The syntheses of **P-2** and **ZnP-2** are shown in Scheme III.6. Suzuki coupling of 5,15-bis(3,5-di-*tert*-butylphenyl)-10-iodo-20-mesitylporphyrin[16] with the pinacol ester of 4-acetylphenyl boronic acid in toluene/DMF (2:1) using $Pd(PPh_3)_4$ (15 mol%) and K_2CO_3 (2 mol equiv) gave **P-2** in 97% yield. Metalation of **P-2** with $Zn(OAc)_2 \cdot 2H_2O$ gave porphyrin **ZnP-2** in 97% yield.

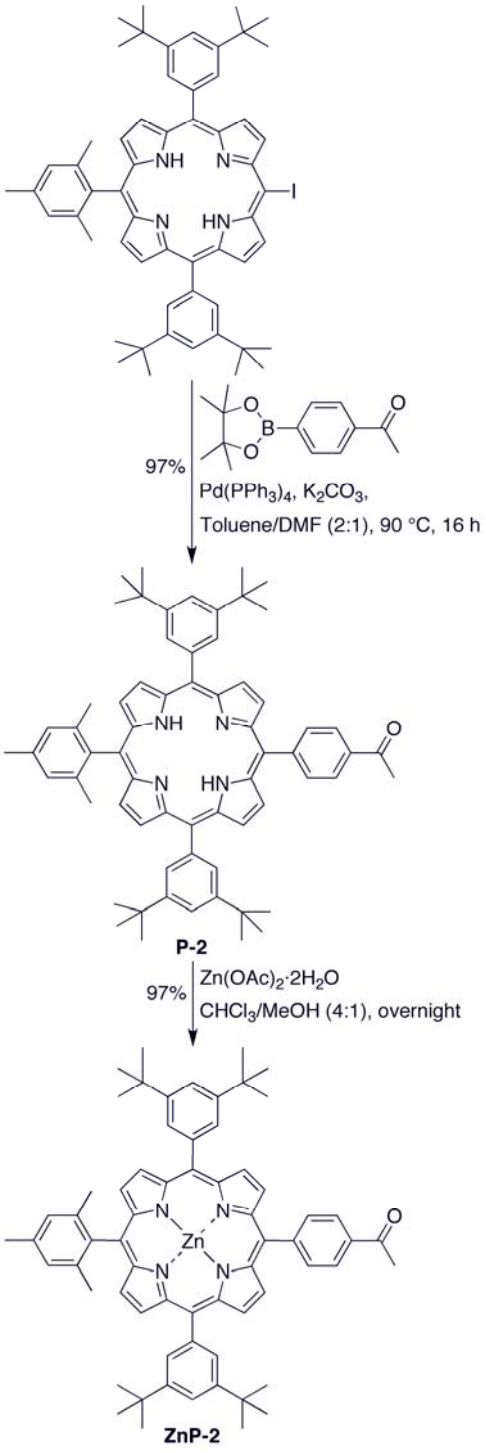

Scheme III.6. Syntheses of **P-2** and **ZnP-2**.

c. Carotenoid-Porphyrin Dyads. The syntheses of **CP-1** and **ZnCP-1** are shown in Scheme III.7. The aldol condensation under microwave irradiation of **P-1** and *trans*-β-apo-8′-carotenal (4 equiv) in the presence of NaOH (10 equiv) in absolute ethanol at 80 °C for 80 minutes afforded **CP-1** in 47% yield (14.6 mg). Metalation of **CP-1** with $Zn(OAc)_2 \cdot 2H_2O$ gave porphyrin **ZnCP-1** in 81% yield (6.4 mg).

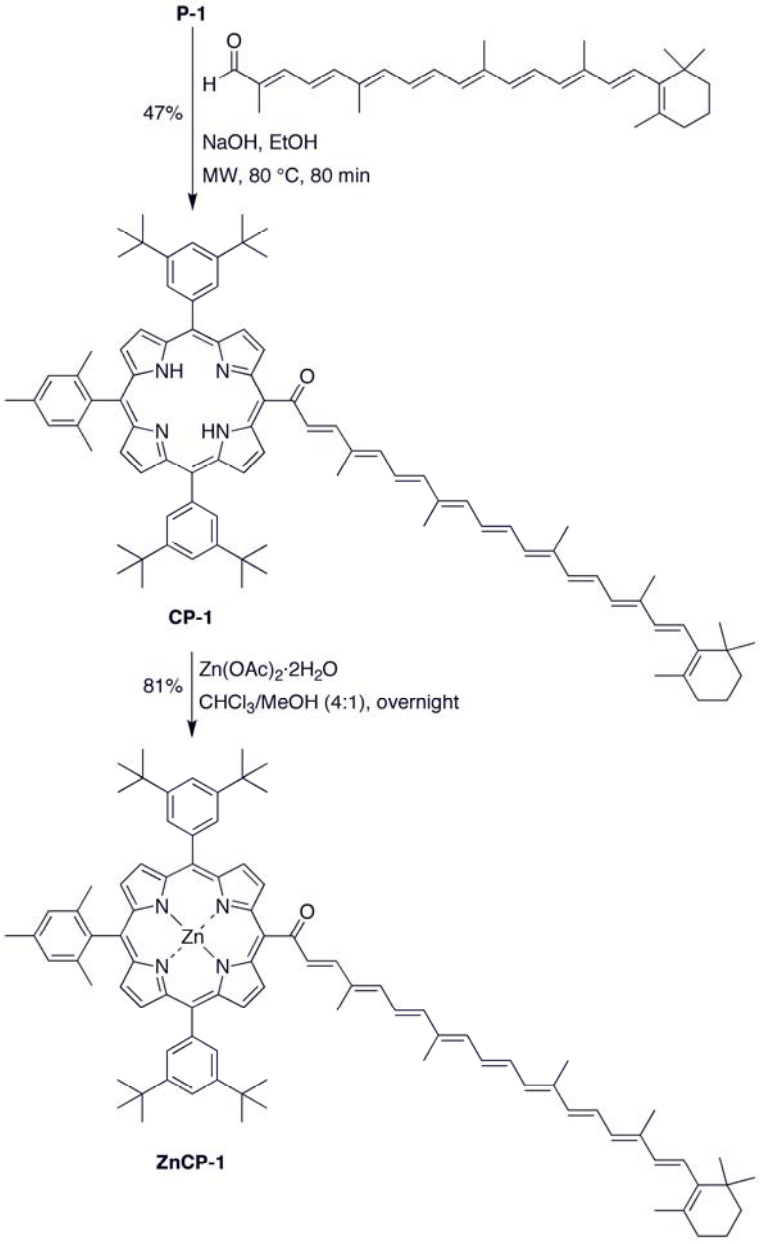

Scheme III.7. Syntheses of **CP-1** and **ZnCP-1**.

The syntheses of **CP-2** and **ZnCP-2** are shown in Scheme III.8. The aldol condensation under microwave irradiation of **P-2** and *trans*-β-apo-8′-carotenal (4 equiv) in

the presence of NaOH (10 equiv) in absolute ethanol at 80 °C for 80 minutes afforded **CP-2** in 48% yield (15.7 mg). Metalation of **CP-2** with $Zn(OAc)_2 \cdot 2H_2O$ gave porphyrin **ZnCP-2** in 92% yield (8.6 mg).

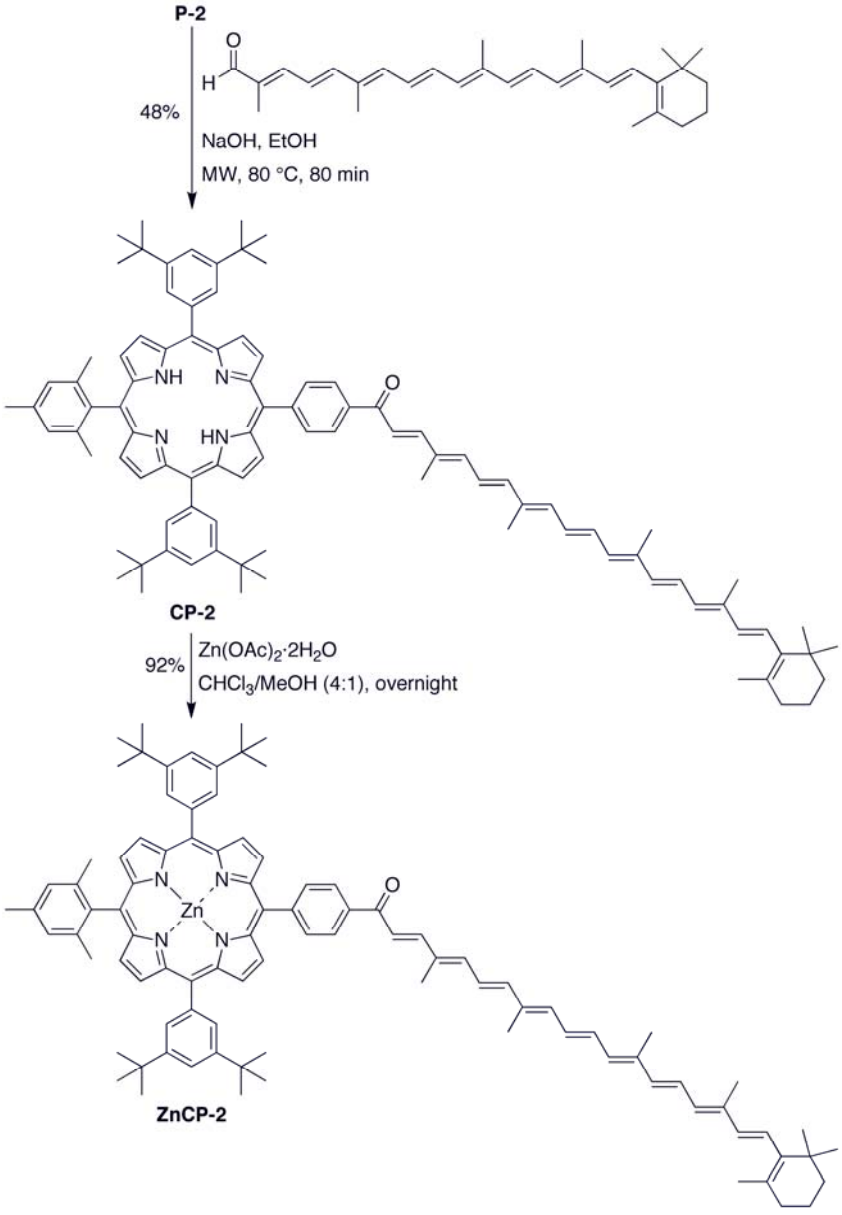

Scheme III.8. Syntheses of **CP-2** and **ZnCP-2**.

2. Characterization a. NMR Spectroscopy. The ^{1}H NMR spectra of the carotenoid-porphyrin dyads have the characteristic features of porphyrins, as well as signals between 6-7 ppm for the majority of the olefin protons. The newly formed double bonds of the observed products were of the (*E*) configuration. The ^{1}H NMR spectrum of **CP-1** contains a doublet at 7.41 ppm with a coupling constant of 15.6 Hz, which is typical of *trans* olefins. Additionally, the ^{1}H NMR spectrum of **ZnCP-2** contains a doublet at 7.72 ppm with a coupling constant of 15.1 Hz.

b. Absorption Spectroscopy. The absorption spectra of the porphyrins, carotenoid-porphyrin dyads, **Car**, and *trans*-β-apo-8′-carotenal were obtained at room temperature in toluene.

The absorption spectra of *trans*-β-apo-8′-carotenal and **Car** are shown in Figure III.2. The absorption spectrum of *trans*-β-apo-8′-carotenal exhibits a broad band with an absorption maximum centered at 468 nm. The product of the aldol condensation of *trans*-β-apo-8′-carotenal with acetophenone (**Car**) exhibits a broad band with an absorption maximum centered at 495 nm. This bathochromic shift is likely due to the increased conjugation in **Car**.

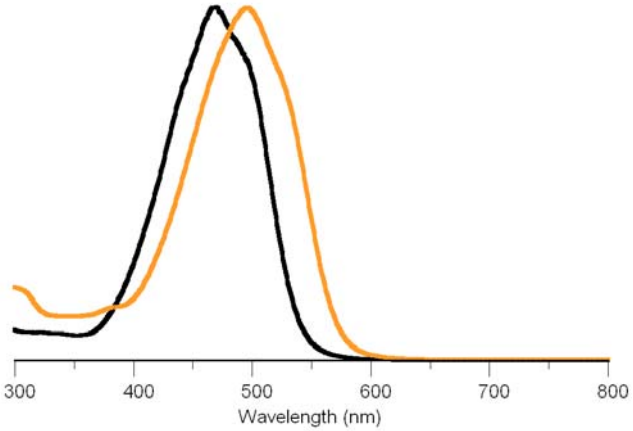

Figure III.2. Absorption spectra in toluene at room temperature of *trans*-β-apo-8′-carotenal (black) and **Car** (orange).

The absorption spectra of **P-1**, **Car**, and **CP-1** are shown in Figure III.3. **P-1** contains a Soret band at 419 nm, as well as weaker Q bands at 515, 548, 591, and 647 nm. **CP-1** has a Soret band at 419 nm, a broad band at 514 nm, and a Q band at 651 nm. The absorption spectrum of **CP-1** contains characteristic features of both **P-1** and **Car**. Figure III.4 shows the residual absorption obtained by subtracting the spectra of **Car** and **P-1** from the spectrum of **CP-1**.

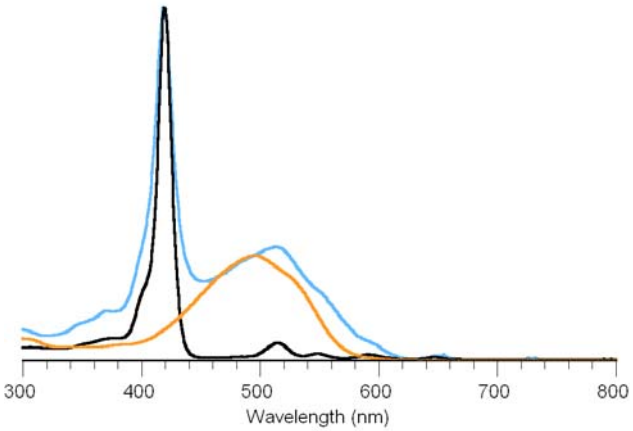

Figure III.3. Absorption spectra in toluene at room temperature of **P-1** (black), **Car** (orange), and **CP-1** (light blue).

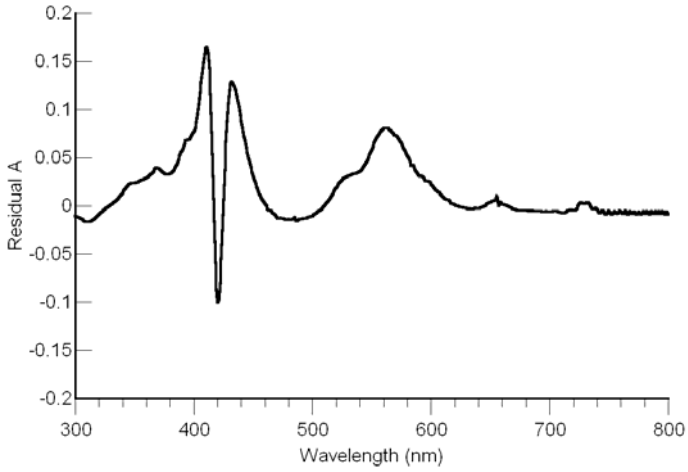

Figure III.4. Residual absorption spectrum obtained by subtracting the spectra of **Car** and **P-1** from the spectrum of **CP-1**. The absorption spectra of **CP-1** and **P-1** were normalized to A=1 at the Soret band. The absorption spectrum of **Car** was normalized to the absorption of **CP-1** at 495 nm.

The absorption spectra of **P-2**, **Car**, and **CP-2** are shown in Figure III.5. **P-2** contains a Soret band at 422 nm, as well as weaker Q bands at 516, 550, 593, and 648 nm. **CP-2** has a Soret band at 422 nm, a broad band at 514 nm, and Q bands at 590 and 649 nm. The

absorption spectrum of **CP-1** contains characteristic features of both **P-2** and **Car**. Figure III.6 shows the residual absorption obtained by subtracting the spectra of **Car** and **P-2** from the spectrum of **CP-2**.

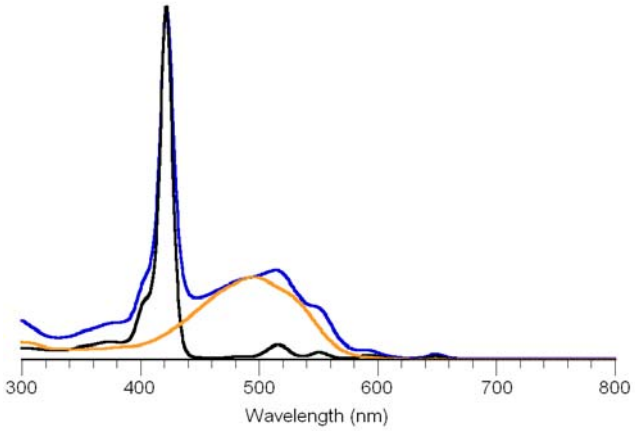

Figure III.5. Absorption spectra in toluene at room temperature of **P-2** (black), **Car** (orange), and **CP-2** (blue).

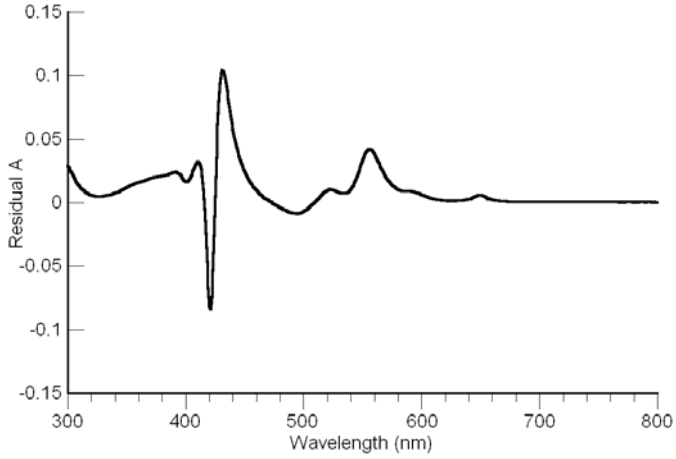

Figure III.6. Residual absorption spectrum obtained by subtracting the spectra of **Car** and **P-2** from the spectrum of **CP-2**. The absorption spectra of **CP-2** and **P-2** were normalized to A=1 at the Soret band. The absorption spectrum of **Car** was normalized to the absorption of **CP-2** at 495 nm.

The absorption spectra of **ZnP-1** and **ZnCP-1** are shown in Figure III.7. The absorption spectrum of **ZnP-1** has a Soret band at 423 nm, as well as weaker Q bands at 550 and 587 nm. **ZnCP-1** has a Soret band at 422 nm, a broad band at 505 nm, and Q bands at 548 and 592 nm. The absorption spectrum of **ZnCP-1** contains characteristic features of both **ZnP-1** and **Car**. Figure III.8 shows the residual absorption obtained by subtracting the spectra of **Car** and **ZnP-1** from the spectrum of **ZnCP-1**.

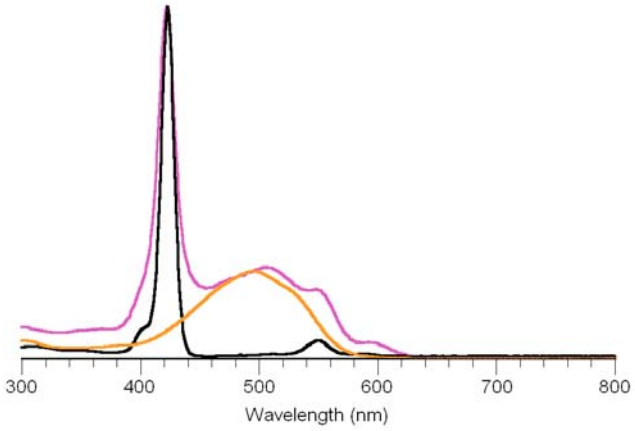

Figure III.7. Absorption spectra in toluene at room temperature of **ZnP-1** (black), **Car** (orange), and **ZnCP-1** (lilac).

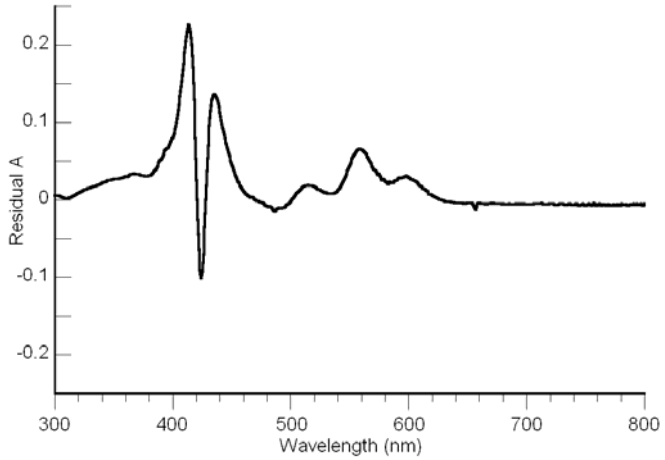

Figure III.8. Residual absorption spectrum obtained by subtracting the spectra of **Car** and **ZnP-1** from the spectrum of **ZnCP-1**. The absorption spectra of **ZnCP-1** and **ZnP-1** were normalized to A=1 at the Soret band. The absorption spectrum of **Car** was normalized to the absorption of **ZnCP-1** at 495 nm.

The absorption spectra of **ZnP-2** and **ZnCP-2** are shown in Figure III.9. **ZnP-2** contains a Soret band at 425 nm, as well as weaker Q bands at 550 and 591 nm. **ZnCP-2** has a Soret band at 425 nm, a broad band at 499 nm, and Q bands at 547 and 588 nm. The absorption spectrum of **ZnCP-2** contains characteristic features of both **ZnP-2** and **Car**. Figure III.10 shows the residual absorption obtained by subtracting the spectra of **Car** and **ZnP-2** from the spectrum of **ZnCP-2**.

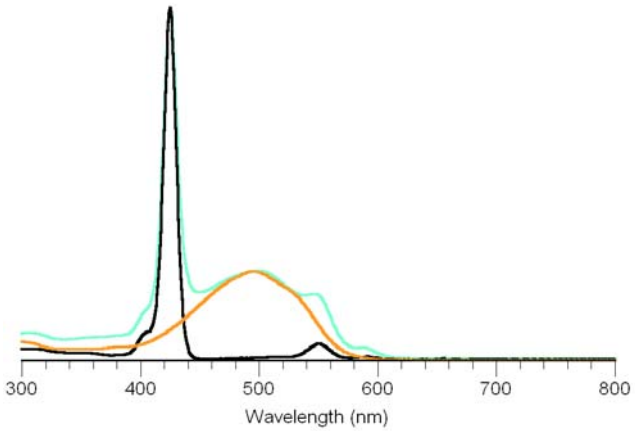

Figure III.9. Absorption spectra in toluene at room temperature of **ZnP-2** (black), **Car** (orange), and **ZnCP-2** (blue-green).

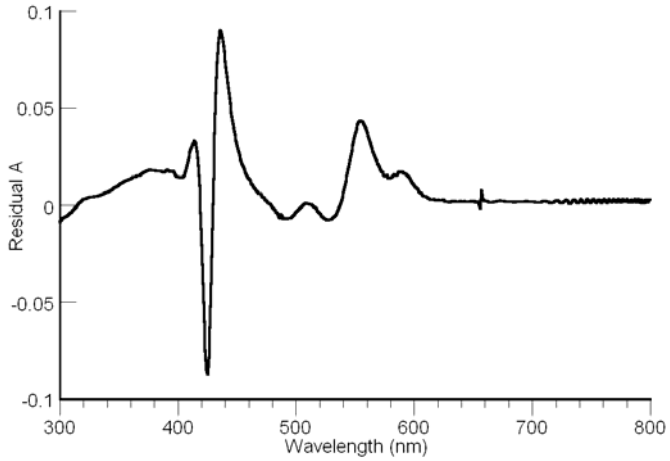

Figure III.10. Residual absorption spectrum obtained by subtracting the spectra of **Car** and **ZnP-2** from the spectrum of **ZnCP-2**. The absorption spectra of **ZnCP-2** and **P-2** were normalized to A=1 at the Soret band. The absorption spectrum of **Car** was normalized to the absorption of **ZnCP-2** at 495 nm.

c. Fluorescence Emission Spectroscopy. The porphyrins were analyzed by fluorescence emission spectroscopy. All spectra were obtained in toluene at room

temperature. The absorption of the Soret band was set to approximately 0.1, and all porphyrins were excited at the wavelength of the Soret band. The fluorescence emission spectra are typical of porphyrins, with Q(0,0) and Q(0,1) bands. All of the emission data are listed in Table III.1.

Table III.1. Emission data of porphyrins and carotenoid-porphyrin dyads.[a]

Porphyrin	λ_{em} (nm) Q(0,0)	λ_{em} (nm) Q(0,1)	$A_{\lambda exc}$
P-1	651	721	0.0985
P-2	654	722	0.0980
ZnP-1	602	650	0.107
ZnP-2	600	650	0.115
CP-1	654	723	0.0824
CP-2	654	725	0.0933
ZnCP-1	610	648	0.0997
ZnCP-2	601	651	0.115

[a] In toluene at room temperature.

The intensity of emission for all of the carotenoporphyrins was less than that for the related benchmark compound (Figures III.11-III.14). This decrease in the intensity of emission may be due to quenching of the excited singlet state of the porphyrin by the carotenoid or through an increase in nonradiative paths to return to the ground state.[5] These compounds will be sent to collaborators to further examine their photophysical properties.

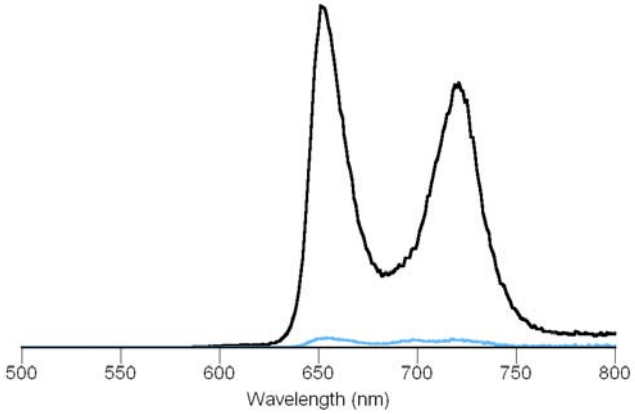

Figure III.11. Fluorescence emission spectra in toluene at room temperature of **P-1** (black) and **CP-1** (light blue). See Table III.1 for the absorbance of the samples at λ_{exc}.

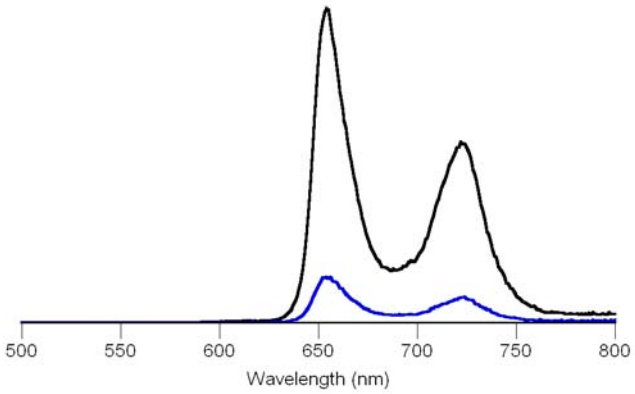

Figure III.12. Fluorescence emission spectra in toluene at room temperature of **P-2** (black) and **CP-2** (blue). See Table III.1 for the absorbance of the samples at λ_{exc}.

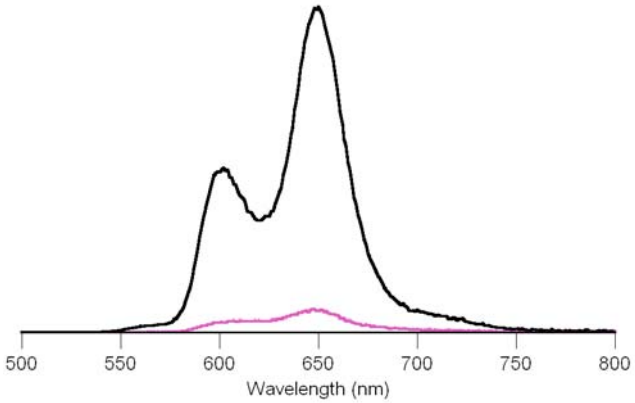

Figure III.13. Fluorescence emission spectra in toluene at room temperature of **ZnP-1** (black) and **ZnCP-1** (violet). See Table III.1 for the absorbance of the samples at λ_{exc}.

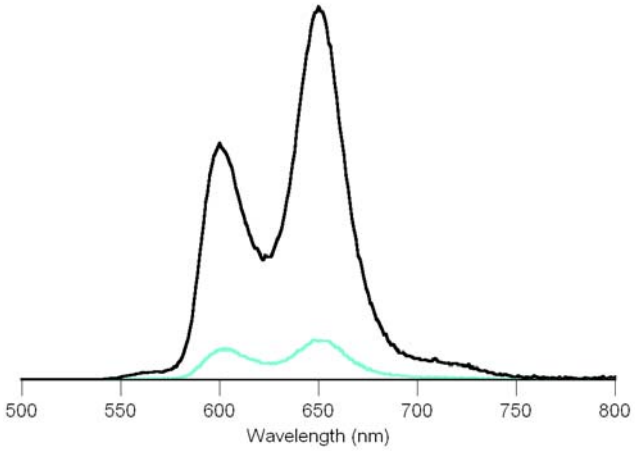

Figure III.14. Fluorescence emission spectra in toluene at room temperature of **ZnP-2** (black) and **ZnCP-2** (blue-green). See Table III.1 for the absorbance of the samples at λ_{exc}.

III.D. Conclusion

The results described herein show that carotenoid-porphyrin dyads can be synthesized in a facile manner by performing an aldol condensation using microwave irradiation. These

carotenoid-porphyrin dyads can be synthesized using the commercially available *trans*-β-apo-8′-carotenal in yields of 47-48%. In each case, the ^{1}H NMR spectrum indicates that the newly formed double bond is of the (*E*) configuration. The absorption spectrum for each carotenoid-porphyrin dyad shows characteristic features of the benchmark carotenoid and the corresponding benchmark porphyrin. Additionally, a decrease in fluorescence emission intensity of each carotenoid-porphyrin dyad versus that of the corresponding benchmark porphyrin was observed. Further photochemical studies will be performed on the compounds by collaborators.

III.E. Experimental Section

General Methods. ^{1}H NMR (300 MHz) spectra were collected at room temperature in $CDCl_3$ unless otherwise noted. Absorption spectra were obtained in toluene at room temperature. All samples were analyzed by laser desorption mass spectrometry (LD-MS) using 1,4-bis-(5-phenyloxazol-2-yl)benzene (POPOP) as the matrix. Electrospray ionization mass spectroscopy (ESI-MS) data are reported for the molecule ion or protonated molecule ion. Silica gel (40 μm average particle size) was used for column chromatography. THF was freshly distilled from sodium/benzophenone ketyl. Anhydrous toluene and DMF were reagent grade and were used as received. The pinacol ester of 4-acetylphenyl boronic acid was purchased from Boron Molecular Inc. (Research Triangle Park, NC). 5,15-Bis(3,5-di-*tert*-butylphenyl)-10-iodo-20-mesitylporphyrin was prepared following a reported procedure.[20]

5-Acetyl-10,20-bis(3,5-di-*tert*-butylphenyl)-15-mesitylporphyrin (P-1). Following a procedure for Stille coupling on chlorins,[17] a mixture of 5,15-bis(3,5-di-*tert*-butylphenyl)-10-iodo-20-mesitylporphyrin (93.1 mg, 0.100 mmol), tributyl(1-ethoxyvinyl)tin (84.5 μL, 0.250 mmol, 2.5 equiv), and $(PPh_3)_2PdCl_2$ (14.0 mg, 0.250 mmol) was refluxed in THF (8.4 mL) for 18 h in a Schlenk flask. The reaction mixture was treated with 10% aqueous HCl (4.8 mL) at room temperature for 2 h. CH_2Cl_2 was added, and the organic layer was separated. The organic layer was washed with saturated aqueous $NaHCO_3$, water, and brine. The organic layer was dried (Na_2SO_4) and concentrated. Column chromatography [silica, CH_2Cl_2/hexanes (1:1) → CH_2Cl_2] afforded a pink-purple solid (53.5 mg, 63%): ^{1}H NMR δ – 2.67 (s, br, 2H), 1.55 (s, 36H), 1.86 (s, 6H), 2.60 (s, 3H), 3.55 (s, 3H), 7.26 (s, 2H), 7.83 (m, 2H), 8.10 (m, 4H), 8.72 (d, *J* = 4.9 Hz, 2H), 8.87 (d, *J* = 4.9 Hz, 2H), 9.03 (d, *J* = 4.9 Hz, 2H), 9.22 (d, *J* = 4.9 Hz, 2H); LD-MS obsd 846.9; ESI-MS obsd *m/z* 847.5294 $(M + H)^+$ corresponds to 846.5221 (M), calcd 846.5237 ($C_{59}H_{66}N_4O$); λ_{abs} 419, 515, 548, 591, 647 nm; λ_{em} (λ_{ex} = 419 nm) 651, 721 nm.

5-(4-Acetylphenyl)-10,20-bis(3,5-di-*tert*-butylphenyl)-15-mesitylporphyrin (P-2). Samples of 5,15-bis(3,5-di-*tert*-butylphenyl)-10-iodo-20-mesitylporphyrin (46.6 mg, 0.0500 mmol), the pinacol ester of 4-acetylphenyl boronic acid (49.2 mg, 0.0500 mmol), anhydrous K_2CO_3 (13.8 mg, 0.100 mmol, 2 equiv) and $Pd(PPh_3)_4$ (8.7 mg, 7.5 μmol, 15 mol%) were weighed into a 10 mL Schlenk flask. The flask was pump-purged with argon three times. Toluene/DMF (5.0 mL, 2:1) was added and the mixture was heated to 90°C under argon. The mixture was stirred for 16 h at 90°C. Column chromatography [silica, CH_2Cl_2/hexanes

(1:1)] afforded a pink-purple solid (44.9 mg, 97%): ^{1}H NMR δ –2.67 (s, br, 2H), 1.53 (s, 36H), 1.87 (s, 6H), 2.62 (s, 3H), 2.88 (s, 3H), 7.28 (s, 2H), 7.79 (m, 2H), 8.09 (m, 4H), 8.71 (d, *J* = 4.9 Hz, 2H), 8.77 (d, *J* = 4.9 Hz, 2H), 8.86 (d, *J* = 4.9 Hz, 2H), 8.90 (d, *J* = 4.9 Hz, 2H); LD-MS obsd 923.4; ESI-MS obsd *m/z* 923.5606 $(M + H)^+$ corresponds to 922.5534 (M), calcd 922.5550 ($C_{65}H_{70}N_4O$); λ_{abs} 422, 516, 550, 593, 648 nm; λ_{em} (λ_{ex} = 421 nm) 654, 722 nm.

5-Acetyl-10,20-bis(3,5-di-*tert*-butylphenyl)-15-mesitylporphinatozinc(II) (ZnP-1). A solution of **P-1** (10.6 mg, 0.0125 mmol) in $CHCl_3$ (4 mL) was treated with a solution of $Zn(OAc)_2{\cdot}2H_2O$ (55.0 mg, 0.250 mmol, 20 equiv) in MeOH (1 mL) and allowed to stir overnight. Column chromatography (silica, CH_2Cl_2) afforded a pink solid (10.2 mg, 90%): ^{1}H NMR δ 1.53 (s, 36H), 1.86 (s, 6H), 2.62 (s, 3H), 3.27 (s, 3H), 7.27 (s, 2H), 7.80 (m, 2H), 8.08 (m, 4H), 8.79 (apparent d, 2H), 8.92 (d, *J* = 4.4 Hz, 2H), 8.97 (d, *J* = 4.9 Hz, 2H); LD-MS obsd 909.2; ESI-MS obsd *m/z* 909.4434 $(M + H)^+$ corresponds to 908.4361 (M), calcd 908.4372 ($C_{59}H_{64}N_4OZn$); λ_{abs} 423, 550, 587 nm; λ_{em} (λ_{ex} = 423 nm) 602, 650 nm.

5-(4-Acetylphenyl)-10,20-bis(3,5-di-*tert*-butylphenyl)-15-mesitylporphinatozinc(II) (ZnP-2). A solution of **P-2** (11.5 mg, 0.0125 mmol) in $CHCl_3$ (4 mL) was treated with a solution of $Zn(OAc)_2{\cdot}2H_2O$ (55.0 mg, 0.250 mmol, 20 equiv) in MeOH (1 mL) and allowed to stir overnight. Column chromatography (silica, CH_2Cl_2) afforded a pink solid (12.0 mg, 97%): ^{1}H NMR δ 1.53 (s, 36H), 1.86 (s, 6H), 2.63 (s, 3H), 2.86 (s, 3H), 7.28 (s, 2H), 7.79 (m, 2H), 8.10 (m, 4H), 8.81 (d, *J* = 4.4 Hz, 2H), 8.87 (d, *J* = 4.9 Hz, 2H), 8.96 (d, *J* = 4.4 Hz, 2H), 9.00 (d, *J* = 4.9 Hz, 2H); LD-MS obsd 985.7; ESI-MS

obsd *m/z* 985.4739 $(M + H)^+$ corresponds to 984.4666 (M), calcd 984.4685 ($C_{65}H_{70}N_4OZn$); λ_{abs} 425, 550, 591 nm; λ_{em} (λ_{ex} = 425 nm) 600, 650 nm.

General Microwave Procedure. A sample of the ketone (1 equiv) was placed in a 125 mL round bottom flask. A magnetic stir bar, aldehyde (4 equiv), NaOH (10 equiv), and absolute ethanol were placed into the flask. The flask was subjected to microwave irradiation at 40 W. The protocol was as follows: (1) Heat from room temperature to 80 °C (irradiation for 2 min), (2) hold at 80 °C (irradiation for 18 min), (3) allow to cool to room temperature (~ 2 min), (4) check the reaction mixture by TLC analysis (silica, toluene), and (5) repeat steps 1-4 until the TLC shows no additional changes. The total irradiation time was 80 minutes (4 cycles). The reaction mixture was concentrated. The resulting crude product was dissolved in CH_2Cl_2 and washed with a saturated aqueous solution of NH_4Cl. The organic layer was separated, dried (Na_2SO_4), and concentrated under reduced pressure.

4,8,13,17-Tetramethyl-1-phenyl-19-(2,6,6-trimethyl-cyclohex-1-enyl)-nonadeca-2,4,6,8,10,12,14,16,18-nonaen-1-one (Car). Following the general procedure with a slight modification, a sample of acetophenone (1.26 mL of a 0.1 M solution in CH_2Cl_2, 0.126 mmol) was placed in a 125 mL round bottom flask and concentrated. A sample of *trans*-β-apo-8′-carotenal (104 mg, 0.252 mmol, 2 equiv) was added to the vessel, as well as NaOH (50.4 mg, 1.26 mmol, 10 equiv), absolute ethanol (75 mL), and a magnetic stir bar. Column chromatography (silica, toluene) followed by a second column [silica, hexanes/CH_2Cl_2 (1:0) → (0:1)] afforded an orange-red solid (38.5 mg, 59%): m.p. 165–167 °C; ^{1}H NMR δ 1.03 (s, 6H), 1.44–1.52 (m, 2H), 1.60–1.68 (m, 2H), 1.72 (s, 3H), 1.95–2.00 (m, 9H), 2.00–2.05 (m,

2H), 2.06 (s, 3H), 6.10–7.00 (m, 13H), 7.44–7.60 (m, 4H), 7.94–8.02 (m, 2H); LD-MS obsd 518.5; ESI-MS not available, calcd 518.3549 ($C_{38}H_{46}O$); λ_{abs} 495 nm (br).

CP-1. Following the general procedure, **P-1** (21.2 mg, 0.0250 mmol), *trans*-β-apo-8′-carotenal (41.7 mg, 0.100 mmol, 4 equiv), NaOH (10.0 mg, 0.250 mmol, 10 equiv), and absolute ethanol (15 mL) were added to a 125 mL round bottom flask. Column chromatography (silica, toluene) followed by a second column [silica, hexanes/CH_2Cl_2 (1:0) → (0:1)] afforded a red-purple solid (14.6 mg, 47%): ^{1}H NMR δ –2.64 (s, br, 2H), 1.01 (s, 6H), 1.40–1.47 (m, 2H), 1.54 (s, 36H), 1.70 (s, 3H), 1.72–1.74 (m, 2H), 1.87 (m, 12H), 1.94 (s, 3H), 1.98–2.02 (m, 2H), 2.08 (s, 3H), 2.63 (s, 3H), 5.92–6.93 (m, 13H), 7.29 (s, 2H), 7.41 (d, *J* = 15.6 Hz, 1H), 7.80 (m, 2H), 8.09 (m, 4H), 8.71 (d, *J* = 4.9 Hz, 2H), 8.86 (d, *J* = 4.9 Hz, 2H), 8.96 (d, *J* = 4.9 Hz, 2H), 9.20 (d, *J* = 4.9 Hz, 2H); LD-MS obsd 1245.8; ESI-MS not available, calcd 1244.8210 ($C_{89}H_{104}N_4O$); λ_{abs} 419, 454 (br), 651 nm; λ_{em} (λ_{ex} = 419 nm) 654, 723 nm, (λ_{ex} = 460 nm) 661, 728 nm.

CP-2. Following the general procedure, **P-2** (23.1 mg, 0.0250 mmol), *trans*-β-apo-8′-carotenal (41.7 mg, 0.100 mmol, 4 equiv), NaOH (10.0 mg, 0.250 mmol, 10 equiv), and absolute ethanol (15 mL) were added to a 125 mL round bottom flask. Column chromatography (silica, toluene) followed by a second column [silica, hexanes/CH_2Cl_2 (1:0) → (0:1)] afforded a red-purple solid (15.7 mg, 48%): ^{1}H NMR δ –2.63 (s, br, 2H), 1.04 (s, 6H), 1.40–1.49 (m, 2H), 1.53 (s, 36H), 1.73 (s, 3H), 1.77–1.80 (m, 2H), 1.87 (s, 6H), 1.99 (s, 6H), 2.02 (s, 3H), 2.07–2.10 (m, 2H), 2.18 (s, 3H), 2.62 (s, 3H), 6.05–6.80 (m, 13H), 7.28 (s, 2H), 7.76-7.82 (m, 3H), 8.10 (m, 4H), 8.36 (s, 4H), 8.71 (d, *J* = 4.9 Hz, 2H), 8.82 (d, *J* = 4.9

Hz, 2H), 8.87 (d, J = 4.9 Hz, 2H), 8.91 (d, J = 4.9 Hz, 2H); LD-MS obsd 1322.9; ESI-MS not available, calcd 1320.8523 ($C_{95}H_{108}N_4O$); λ_{abs} 422, 514 (br), 649 nm; λ_{em} (λ_{ex} = 422 nm) 654, 725 nm, (λ_{ex} = 460 nm) 652, 726 nm.

ZnCP-1. A solution of **CP-1** (7.5 mg, 0.0060 mmol) in $CHCl_3$ (4 mL) was treated with a solution of $Zn(OAc)_2{\cdot}2H_2O$ (13.2 mg, 0.0600 mmol, 20 equiv) in MeOH (1 mL) and allowed to stir overnight. Column chromatography [silica, hexanes/CH_2Cl_2 (1:1)] afforded a red-purple solid (6.4 mg, 81%): ^{1}H NMR (CD_2Cl_2) δ 1.05 (m, 6H), 1.40–1.42 (m, 4H), 1.53 (s, 36H), 1.68 (s, 2H), 1.74 (s, 3H), 1.88 (m, 3H), 1.93 (s, 3H), 2.00 (m, 3H), 2.67 (s, 3H), 5.95–6.750 (m, 14H), 7.36 (s, br, 2H), 7.84 (m, 2H), 8.09 (s, br, note 1) 8.37 (s, br, note 1), 8.79 (d, J = 4.7 Hz, 2H), 8.83 (d, J = 4.7 Hz, 2H); LD-MS obsd 1308.0; ESI-MS not available, calcd 1306.7345 ($C_{89}H_{102}N_4OZn$); λ_{abs} 422, 505 (br), 548, 592 nm; λ_{em} (λ_{ex} = 422 nm) 610, 648 nm. Note 1: Some of the signals are very broad, which makes accurate integration difficult.

ZnCP-2. A solution of **CP-2** (8.9 mg, 0.00675 mmol) in $CHCl_3$ (4 mL) was treated with a solution of $Zn(OAc)_2{\cdot}2H_2O$ (14.8 mg, 0.0675 mmol, 20 equiv) in MeOH (1 mL) and allowed to stir overnight. Column chromatography [silica, hexanes/CH_2Cl_2 (1:1)] afforded a red-purple solid (8.6 mg, 92%): ^{1}H NMR δ 1.04 (m, 6H), 1.27–1.41 (m, 2H), 1.53 (s, 36H), 1.60-1.68 (m, 2H), 1.70-1.78 (m, 2H), 1.87 (s, 6H), 1.99 (s, 3H), 2.02 (m, 9H), 2.17 (s, 3H), 2.63 (s, 3H), 6.10–6.80 (m, 13H), 7.28 (s, 2H), 7.72 (d, J = 15.1 Hz, 1H), 7.79 (m, 2H), 8.11 (m, 4H), 8.34 (m, 4H), 8.81 (d, J = 4.9 Hz, 2H), 8.91 (d, J = 4.9 Hz, 2H), 8.96 (d, J = 4.9 Hz,

2H), 9.00 (d, J = 4.9 Hz, 2H); LD-MS obsd 1384.2; ESI-MS not available, calcd 1382.7658 ($C_{95}H_{106}N_4OZn$); λ_{abs} 425, 499 (br), 547, 588 nm; λ_{em} (λ_{ex} = 425 nm) 601, 651 nm.

III.F. References

(1) Blankenship, R. E. *Molecular Mechanisms of Photosynthesis.* Blackwell Science: Oxford, 2002; Chapter 1.

(2) Yu, L.; Lindsey, J. S. *J. Org. Chem.* **2001**, *66*, 7402–7419.

(3) Blankenship, R. E. *Molecular Mechanisms of Photosynthesis.* Blackwell Science: Oxford, 2002; Chapter 5.

(4) Blankenship, R. E. *Molecular Mechanisms of Photosynthesis.* Blackwell Science: Oxford, 2002; Chapter 4.

(5) Gust, D; Moore, T. A.; Moore, A. L.; Devadoss, C.; Liddell, P. A.; Hermant, R.; Nieman, R. A.; Demanche, L. J.; DeGraziano, J. M.; Gouni, I. *J. Am. Chem. Soc.* **1992**, *114*, 3590–3603.

(6) Demmig-Adams, B.; Adams, W. W. III *Trends Plant Sci.* **1996**, *1*, 21–26.

(7) Bensasson, R. V.; Land, E. J.; Moore, A. L.; Crouch, R. L.; Dirks, G.; Moore, T. A.; Gust, D. *Nature* **1981**, *290*, 329–332.

(8) (a) Effenberger, F.; Schlosser, H.; Bäuerle, P.; Maier, S.; Port, H; Wolf, H. C. *Angew. Chem. Int. Ed. Engl.* **1988**, *26*, 281–284. (b) Momenteau, M.; Loock, B.; Seta, P.; Bienvenue, E.; d'Epenoux, B. *Tetrahedron* **1989**, *45*, 4893–4901.

(9) Hermant, R. M.; Liddell, P. A.; Lin, S.; Alden, R. G.; Kang, H. K.; Moore, A. L.; Moore, T. A.; Gust, D. *J. Am. Chem. Soc.* **1993**, *115*, 2080–2081.

(10) Tatman, D.; Liddell, P. A.; Moore, T. A.; Gust, D.; Moore, A. L. *Photochem. Photobiol.* **1998**, *68*, 459–466.

(11) Gust, D.; Moore, T. A.; Bensasson, R. V.; Mathis, P.; Land, E. J.; Chachaty, C.; Moore, A. L.; Liddell, P. A.; Nemeth, G. A. *J. Am. Chem. Soc.* **1985**, *107*, 3631–3640.

(12) Gust, D.; Moore, T. A.; Moore, A. L.; Liddell, P. A. *Methods Enzymol.* **1992**, *213*, 87–100.

(13) Fungo, F.; Otero, L.; Durantini, E.; Thompson, W. J.; Silber, J. J.; Moore, T. A.; Moore, A. L.; Gust, D.; Sereno, L. *Phys. Chem. Chem. Phys.* **2003**, *5*, 469–475.

(14) Osuka, A.; Yamada, H.; Maruyama, K. *Chem. Lett.* **1990**, 1905–1908.

(15) Ruzié , C.; Krayer, M.; Lindsey, J. S. *Org. Lett.* **2009**, *11*, 1761–1764.

(16) Yu, L.; Lindsey, J. S. *Tetrahedron* **2001**, *57*, 9285–9298.

(17) Laha, J. K.; Muthiah, C.; Taniguchi, M.; McDowell, B. E.; Ptaszek, M.; Lindsey, J. S. *J. Org. Chem.* **2006**, *71*, 4092–4102.